Star formation

Outflows and jets

Observations of outflows and jets

- Optically detected jets:
  - Very collimated streams of gas, moving at supersonic speed (~100 km/s)
  - Mostly bipolar, mostly perpendicular to disk

Jet outflow rate typically 10^{-9}... 10^{-7} $M_{\odot}$.

- Molecular outflows:
  - Detected in CO lines
  - Less colimated
  - Often associated with optical jets (i.e. same origin)

Derived mass: 0.1...170 $M_{\odot}$: large!

- Most of accelerated mass must have been swept up from the cloud core, rather than originating in mass ejected from the star

Herbig-Haro objects

Most prominent outflow products

- Radiation from excited hydrogen
- Shock interaction of jet with surrounding cloud

HH 1 and 2

Jet powered by the embedded source VLA1

green: Hα, red: SII

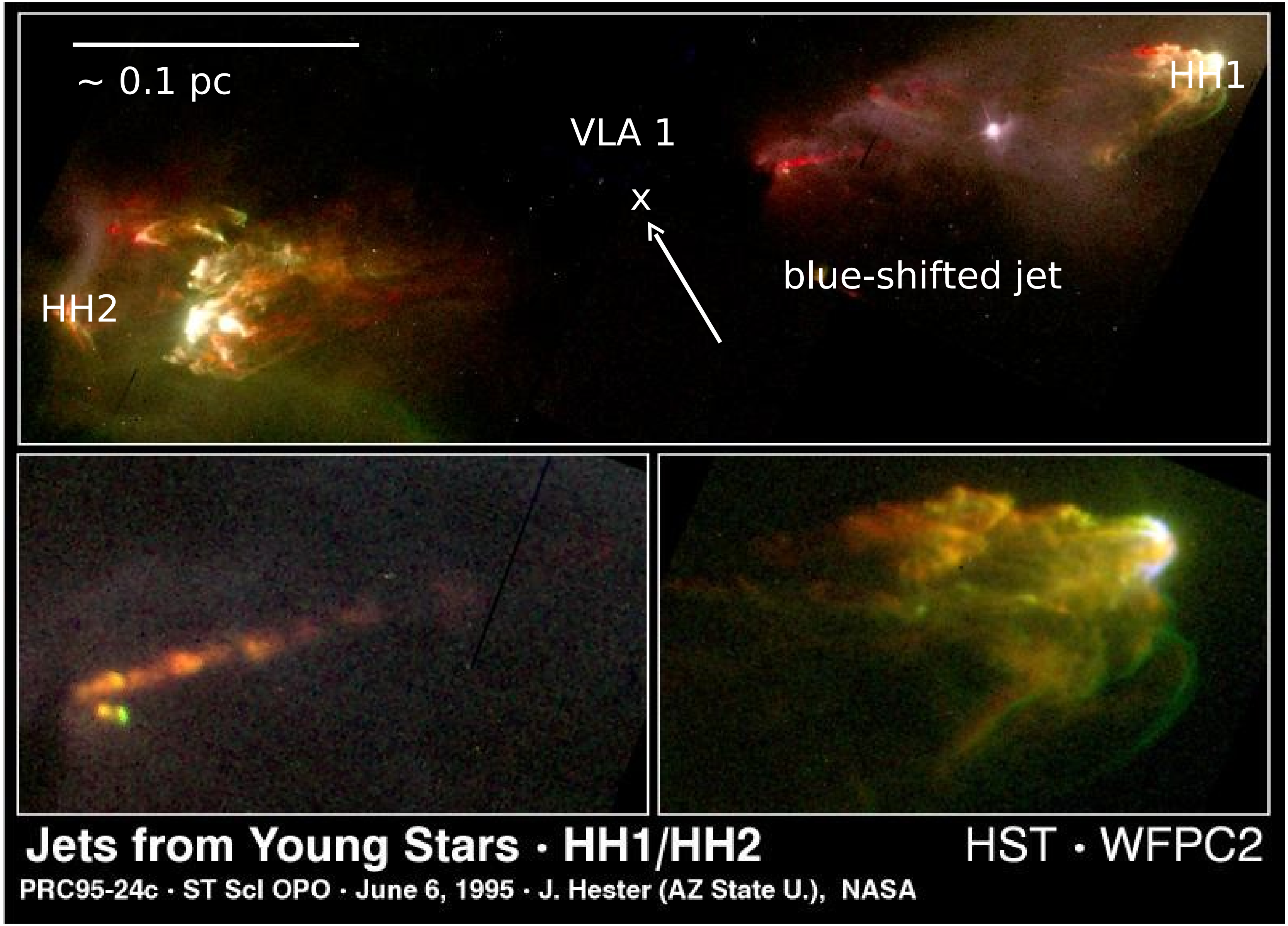

Jets are observable in lines of ionized atoms

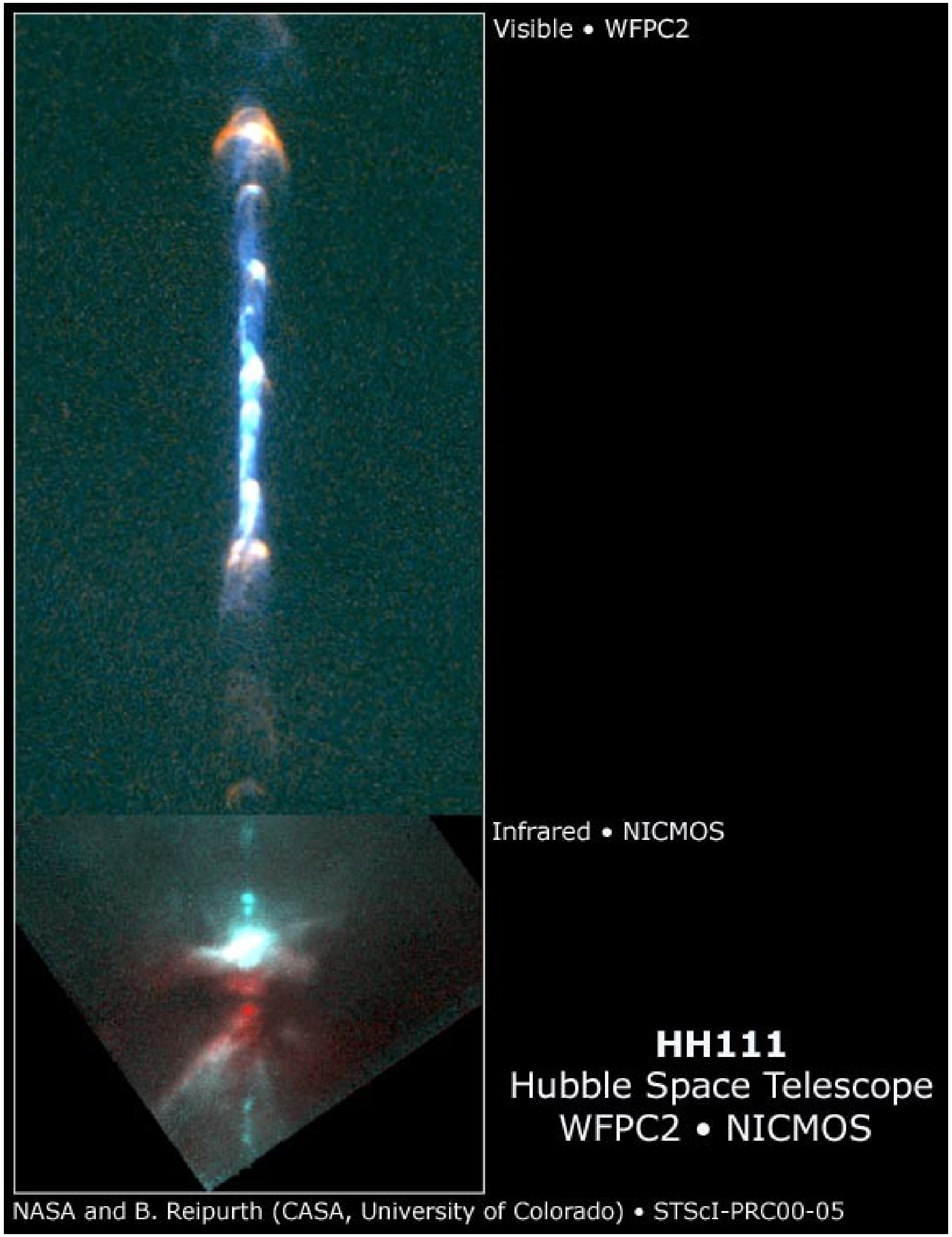

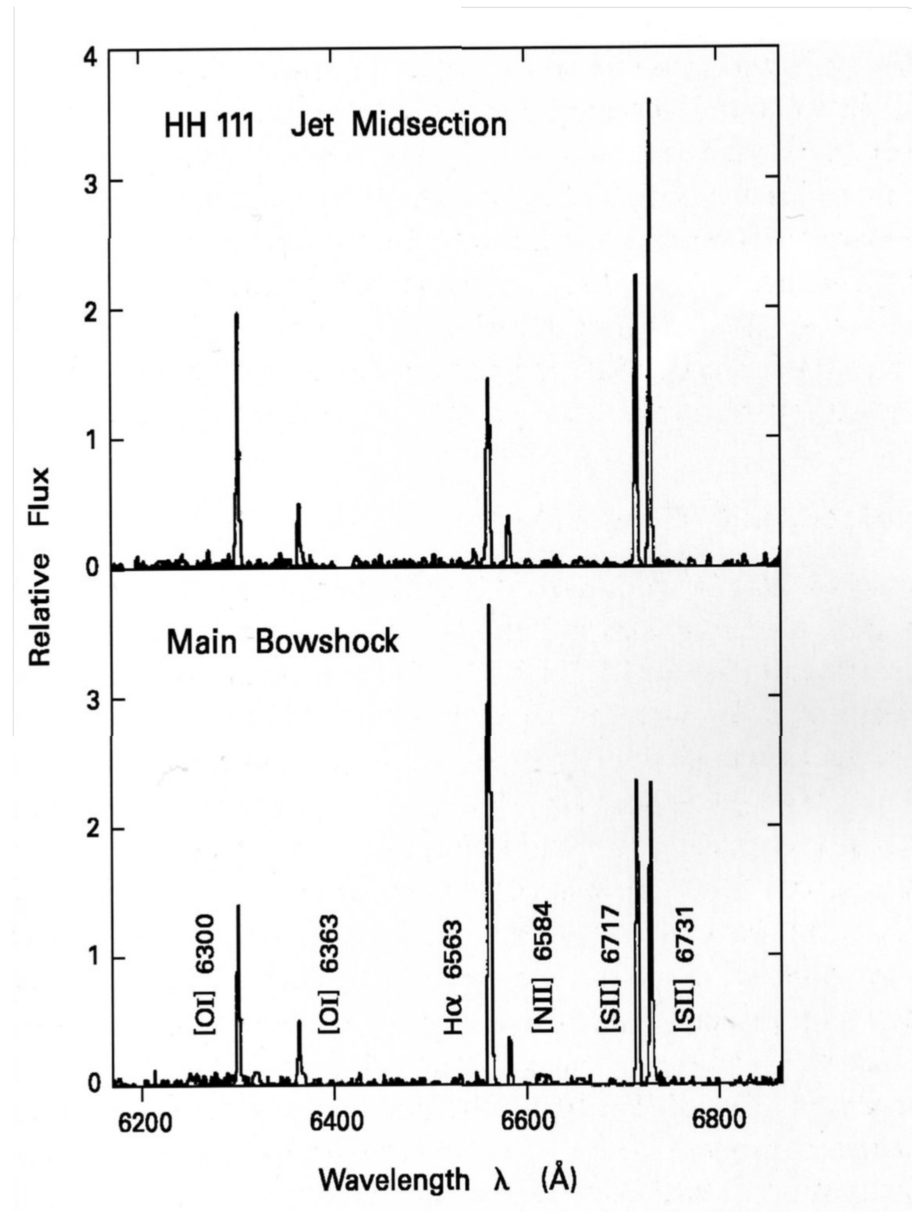

HH 34

HH 47

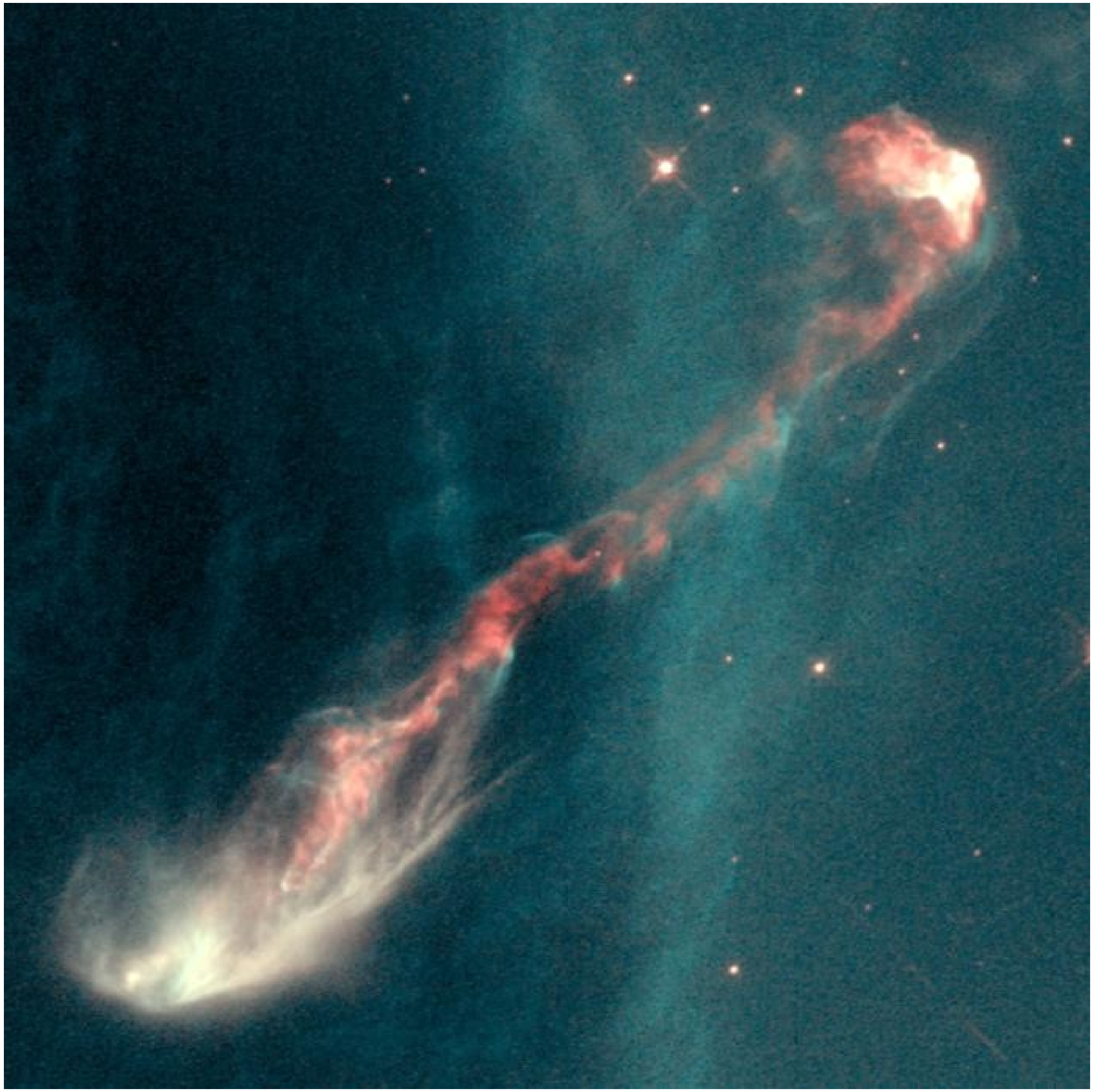

HH 30

First direct observation of temporal changes

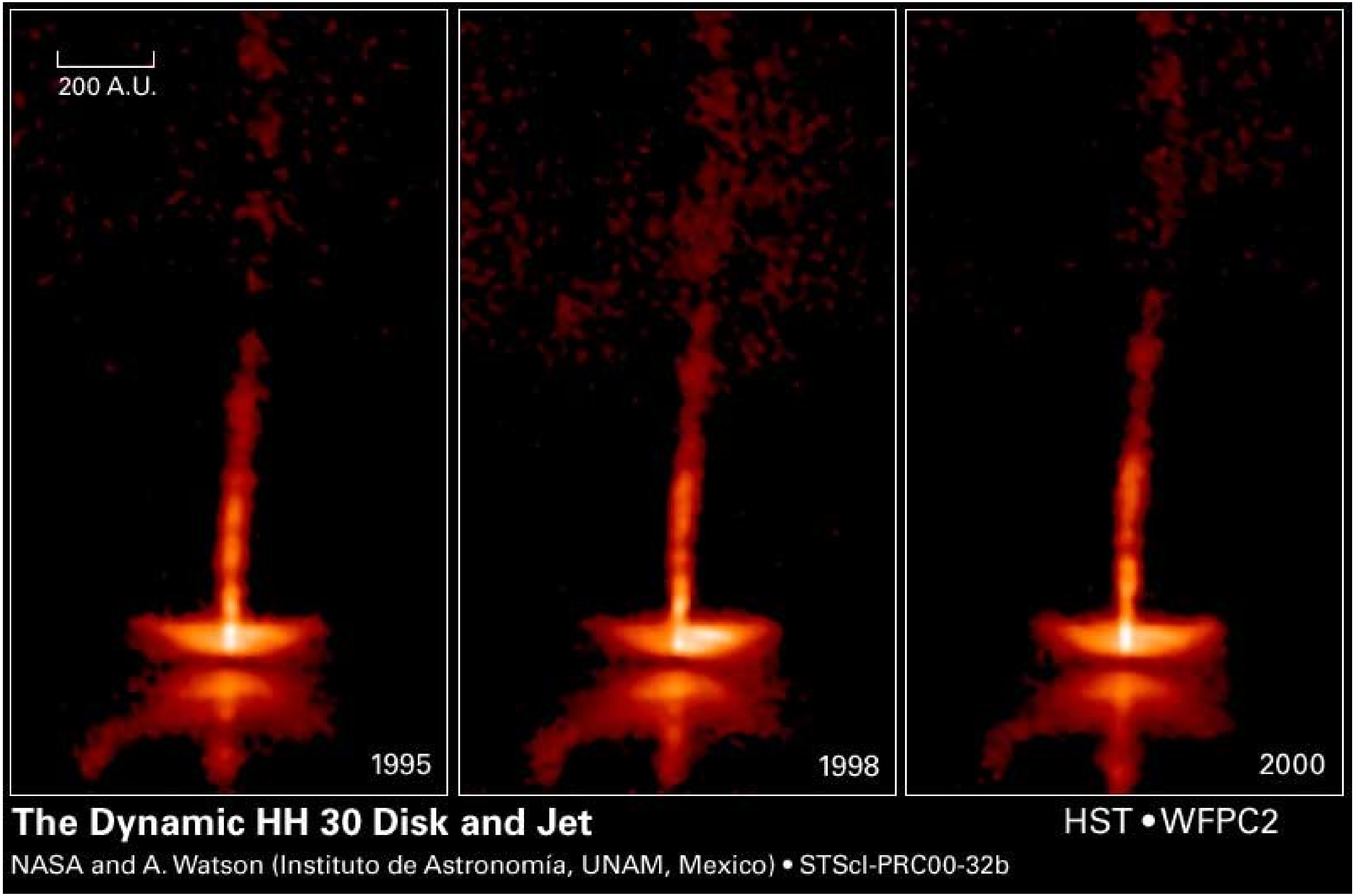

HH 30

Association with molecular gas in disk and outflow

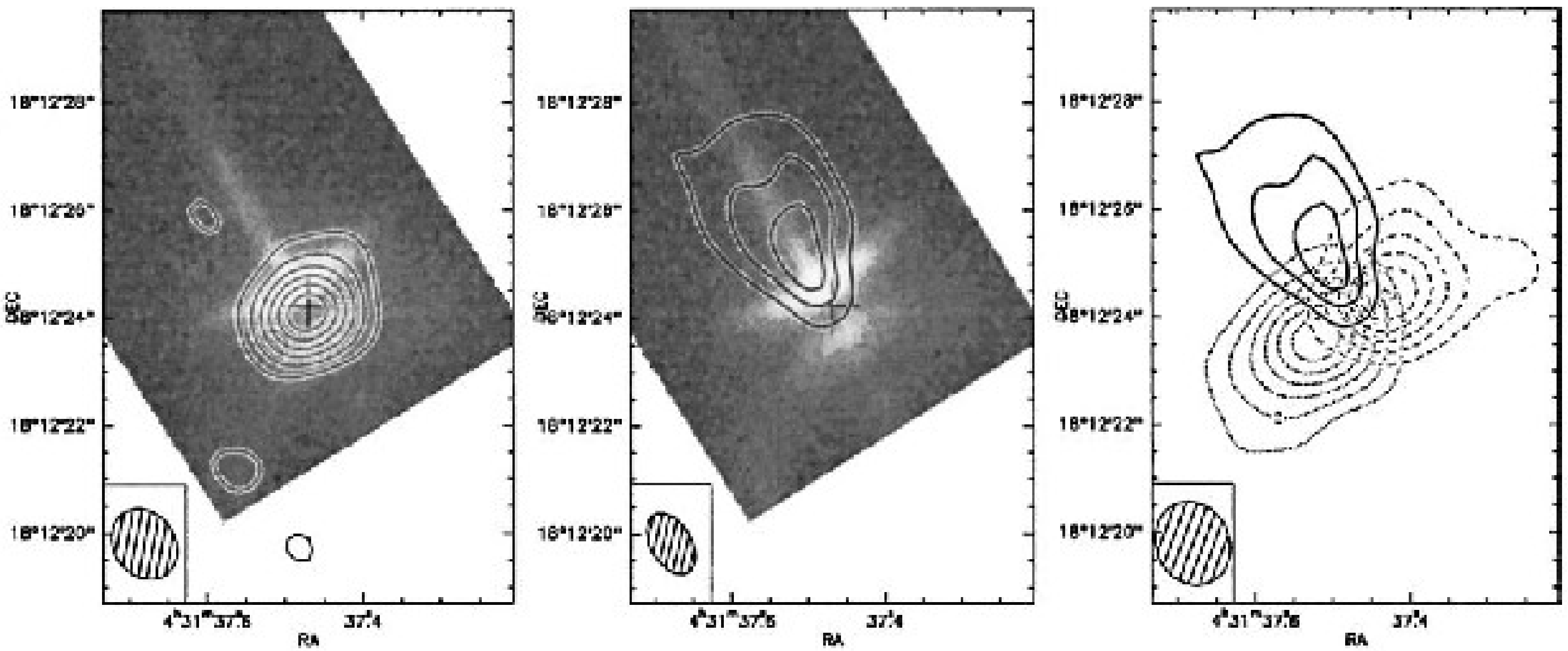

Figure 2. Background in false color: a montage of the dust disk emission from the HST (from Burrows et al., 1996) and its perpendicular jet. Contours present ^{12}CO J $= 2-1$ emission associated to the jet (black and white) corresponding to the extreme velocities and the redshifted and blueshifted integrated emission with respect to the systemic velocity of ^{13}CO J $= 2-1$ line coming from the disk (from Pety et al., 2004). Note that the velocity gradient of the ^{13}CO J $= 2-1$ emission is along the major disk axis, as expected for rotation.

HH211: a well collimated low mass flow

- Many jets only detected in the Infrared
- Complementary CO observations “fill” the outflow pattern

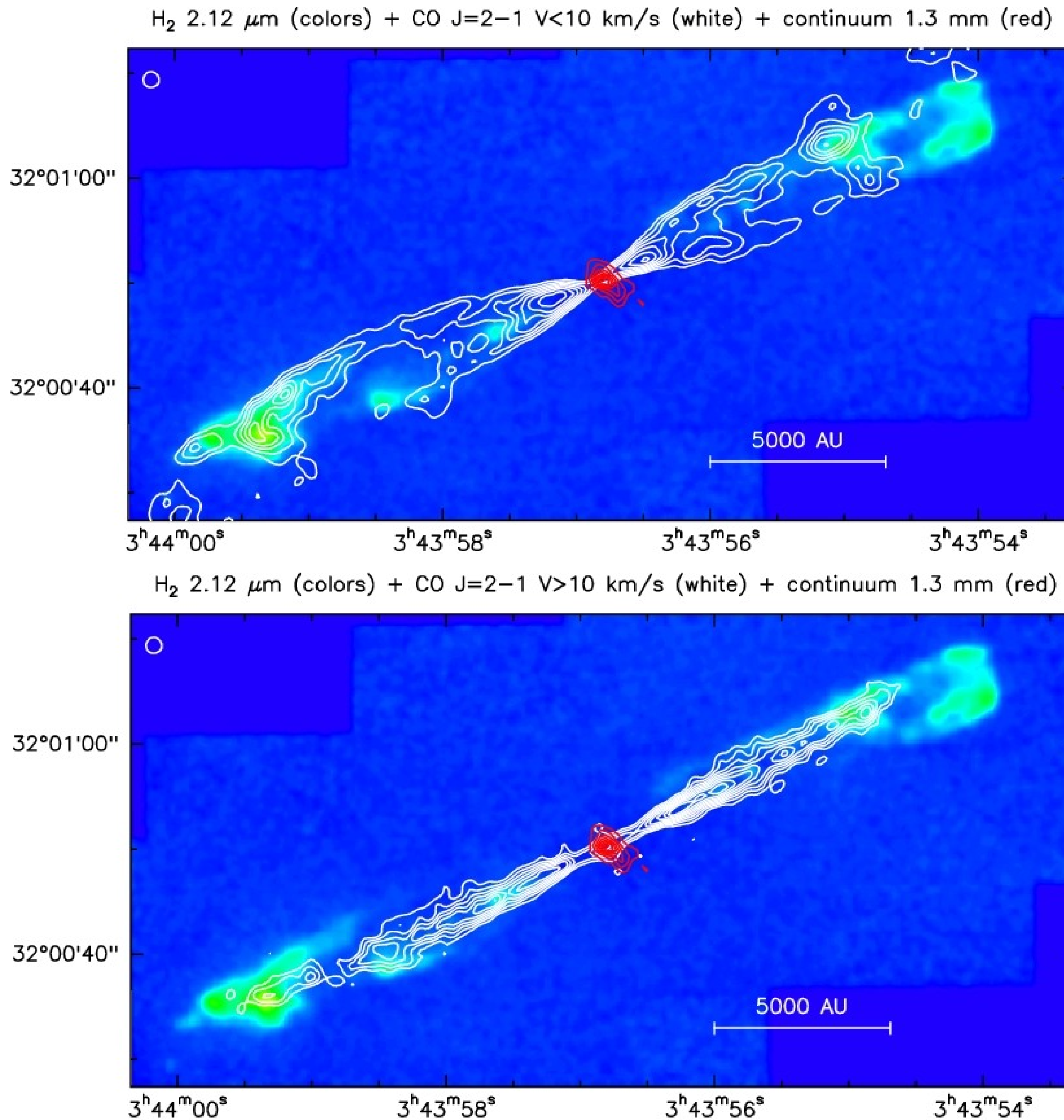

HH 212

Dragon

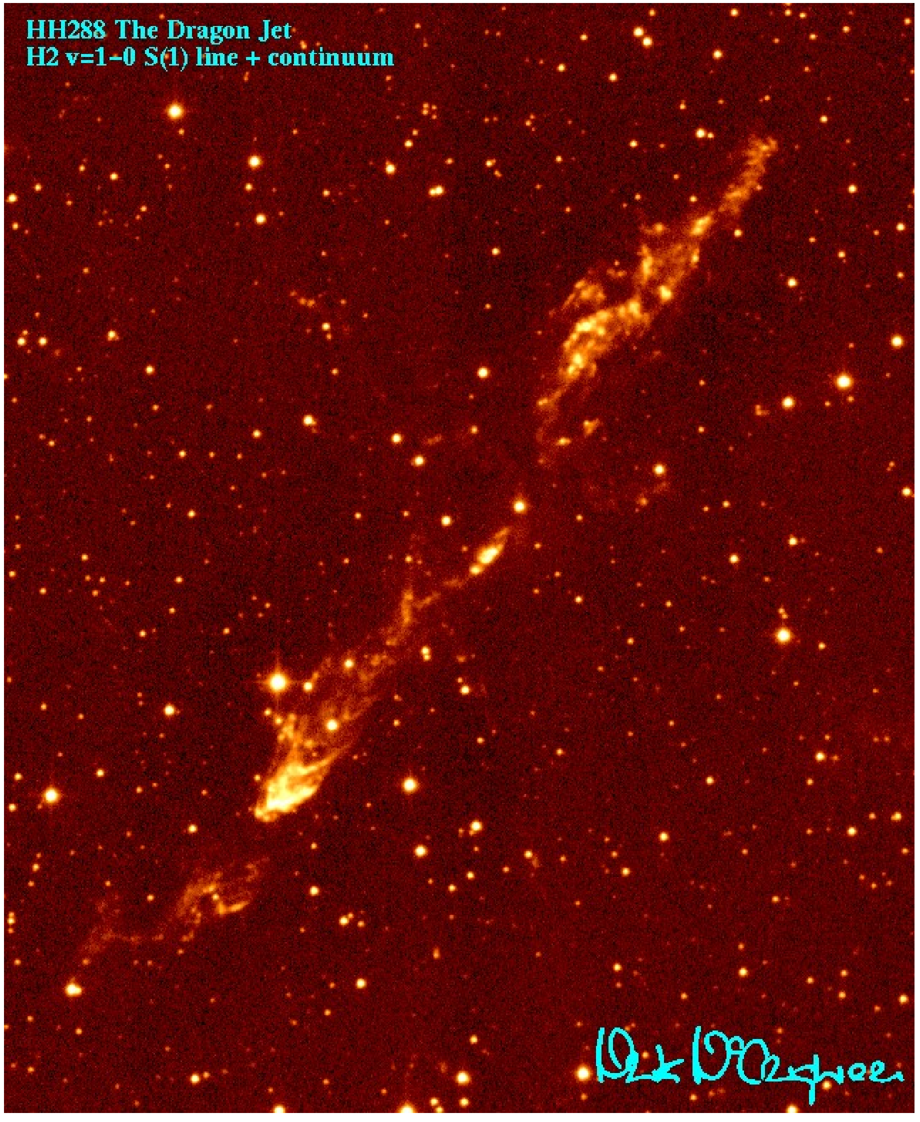

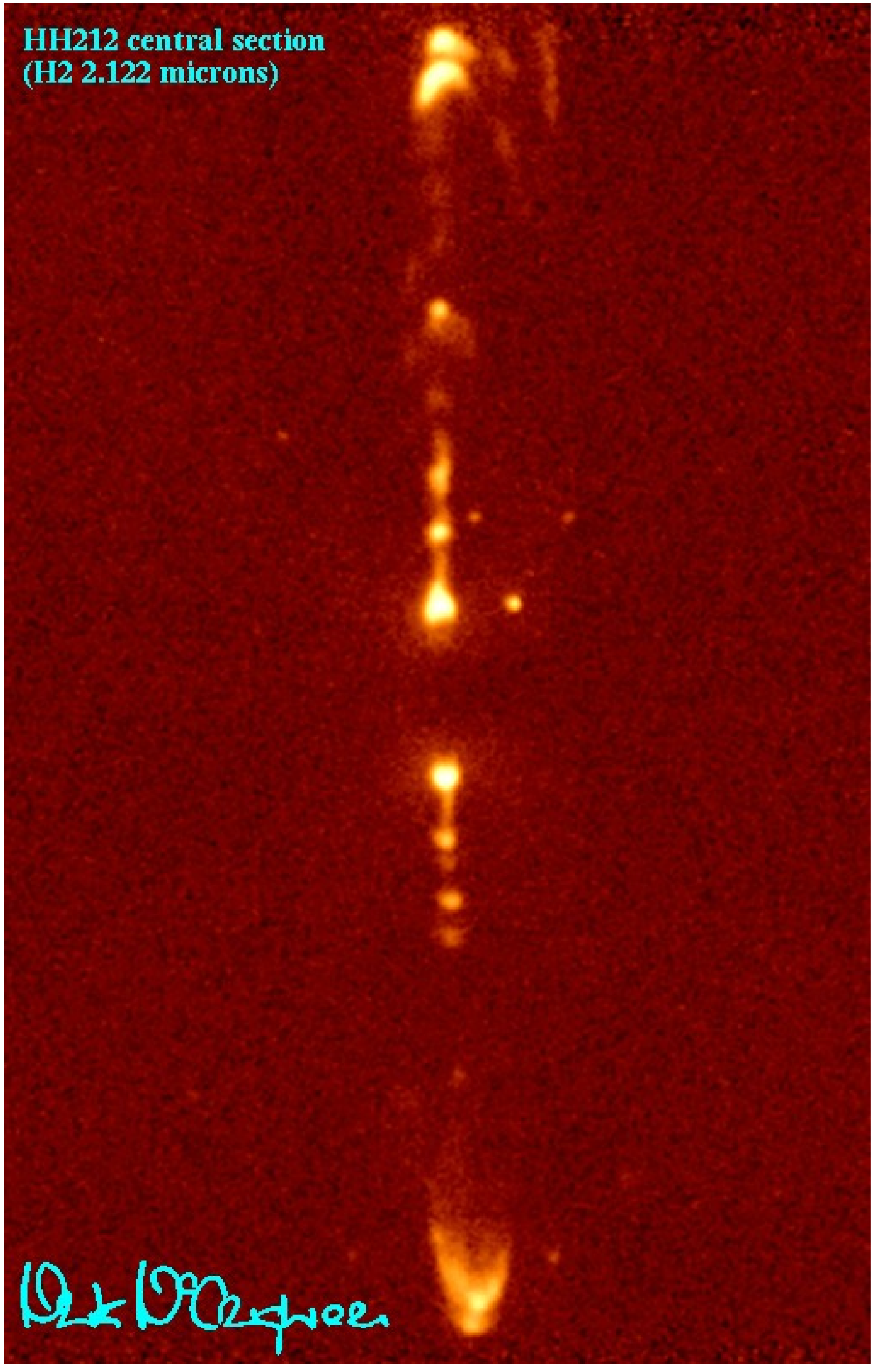

The BHR71 Bok globule

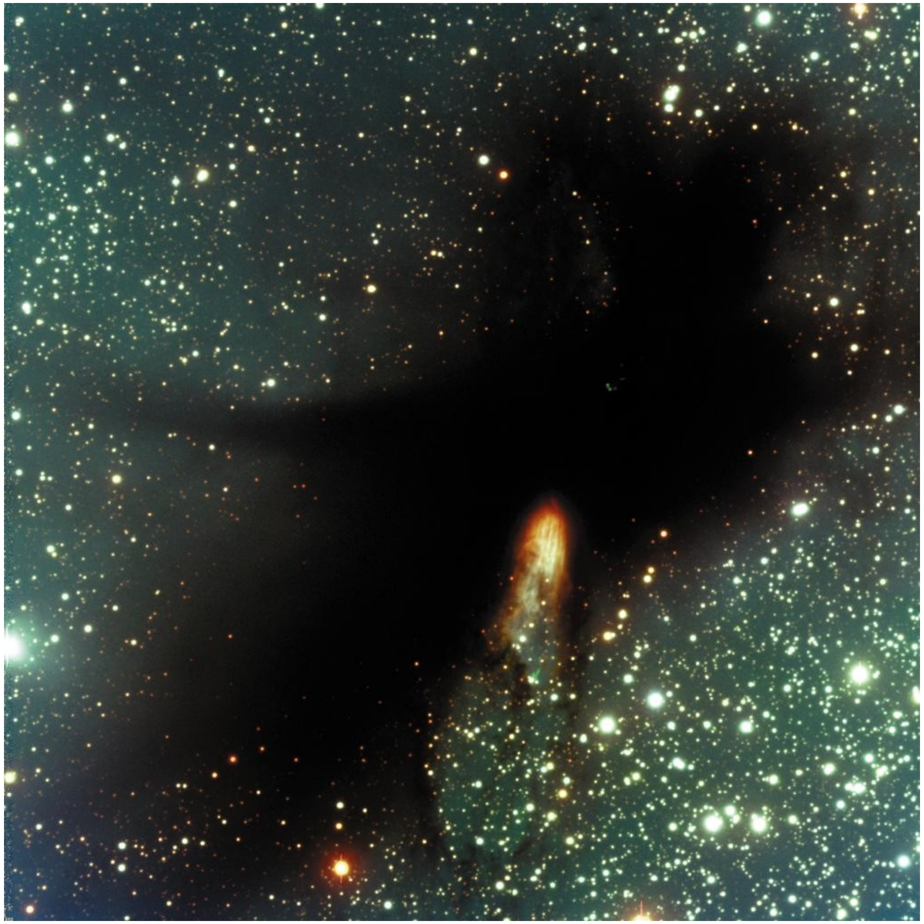

© J. Alves et al. (ESO Messenger 103)

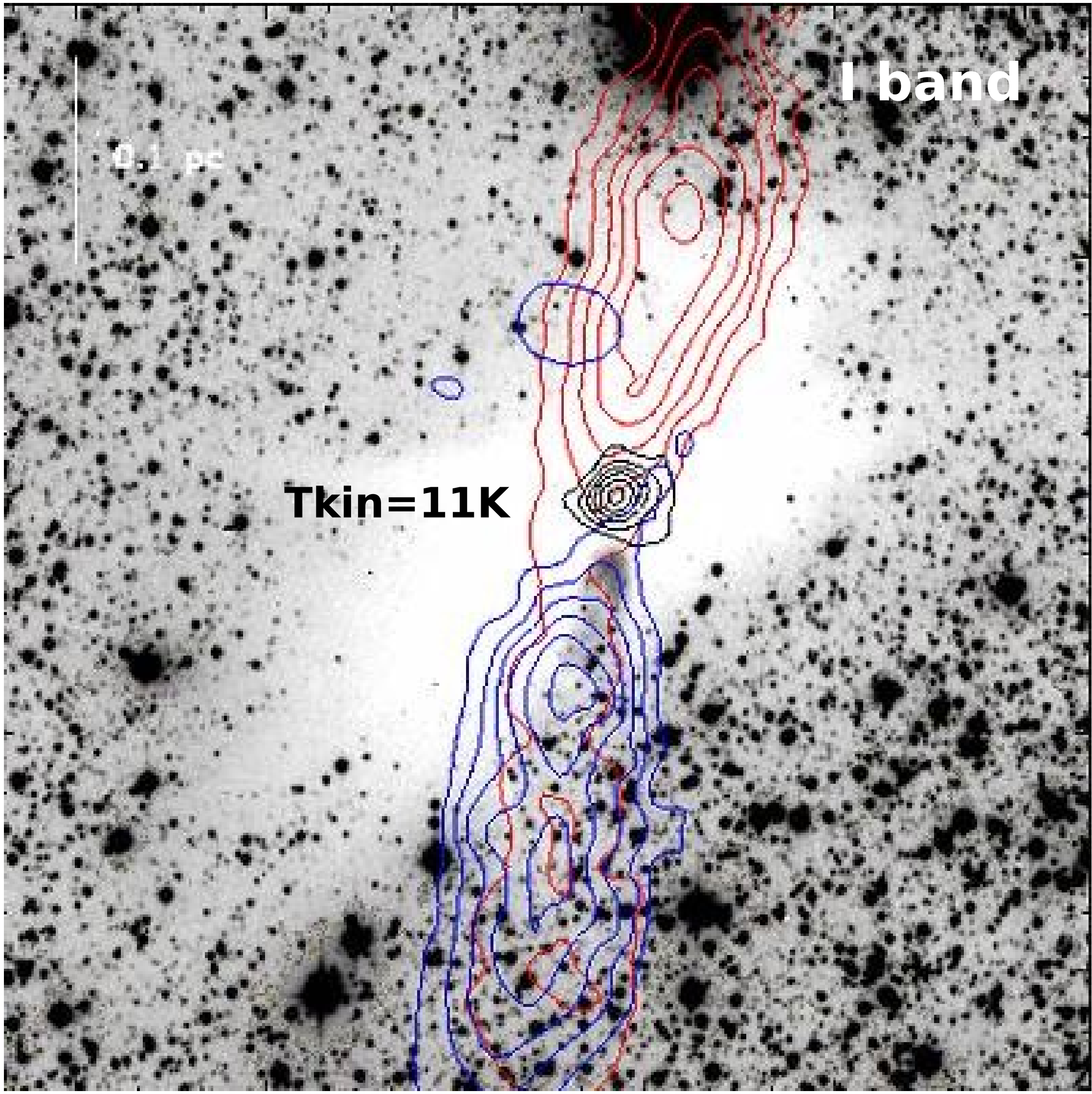

CO (1-0) outflow, powered by a class 0 protostellar binary ($L_{bol} \sim 9\ L_{\odot}$)

Bourke et al. (1997)

Mapping of the outflow with APEX

APEX -
Chajnant

CO(3-2)

Parise et al. 2006

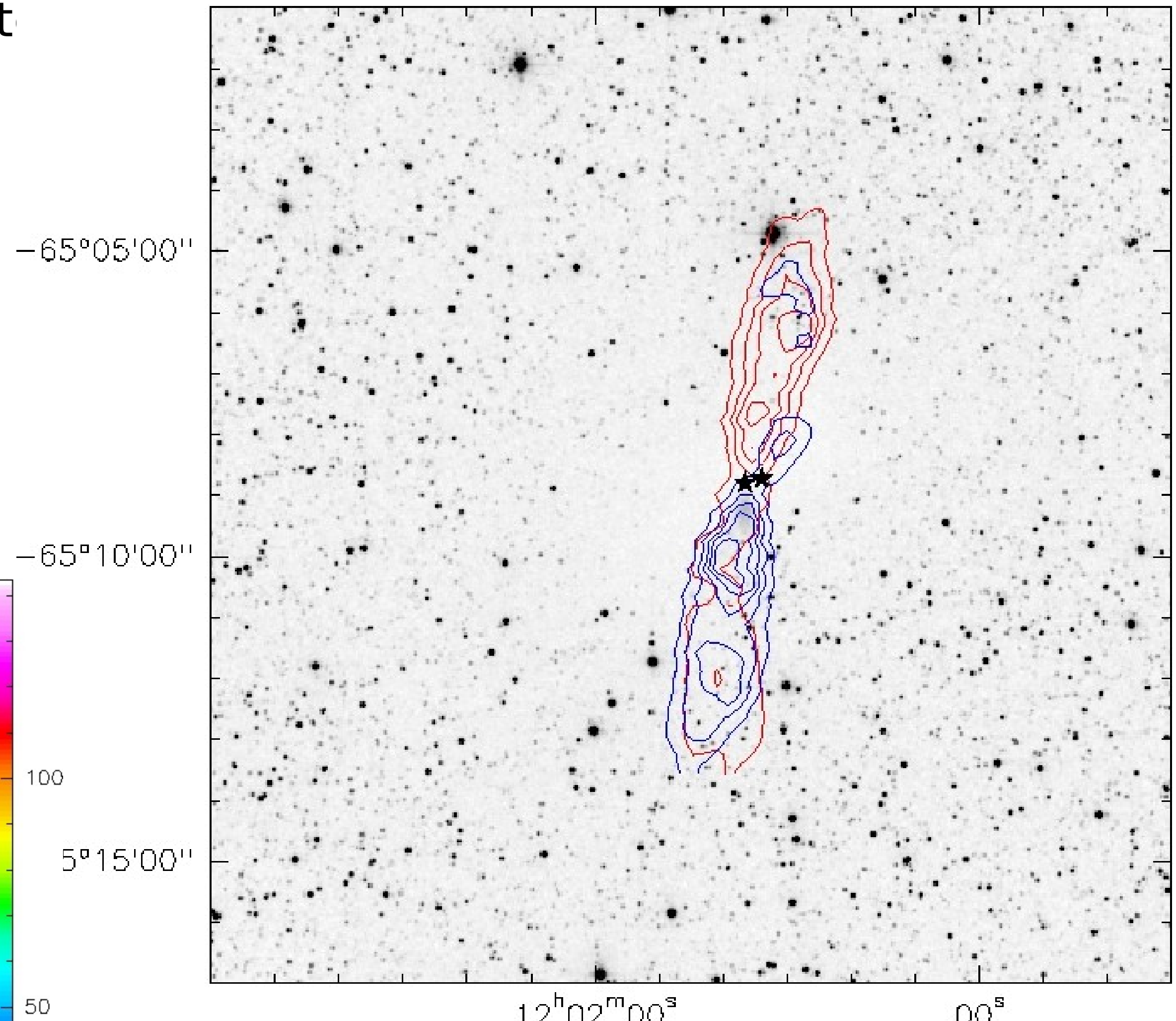

2MASS J band image

IRAS 11590-6452:
a binary
protostellar system
(ISO observations,
Myers & Mardones
1998)

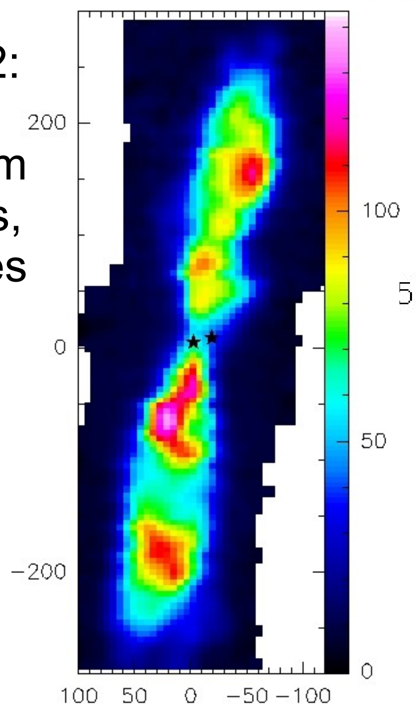

CO(3-2) channel maps

redshifted

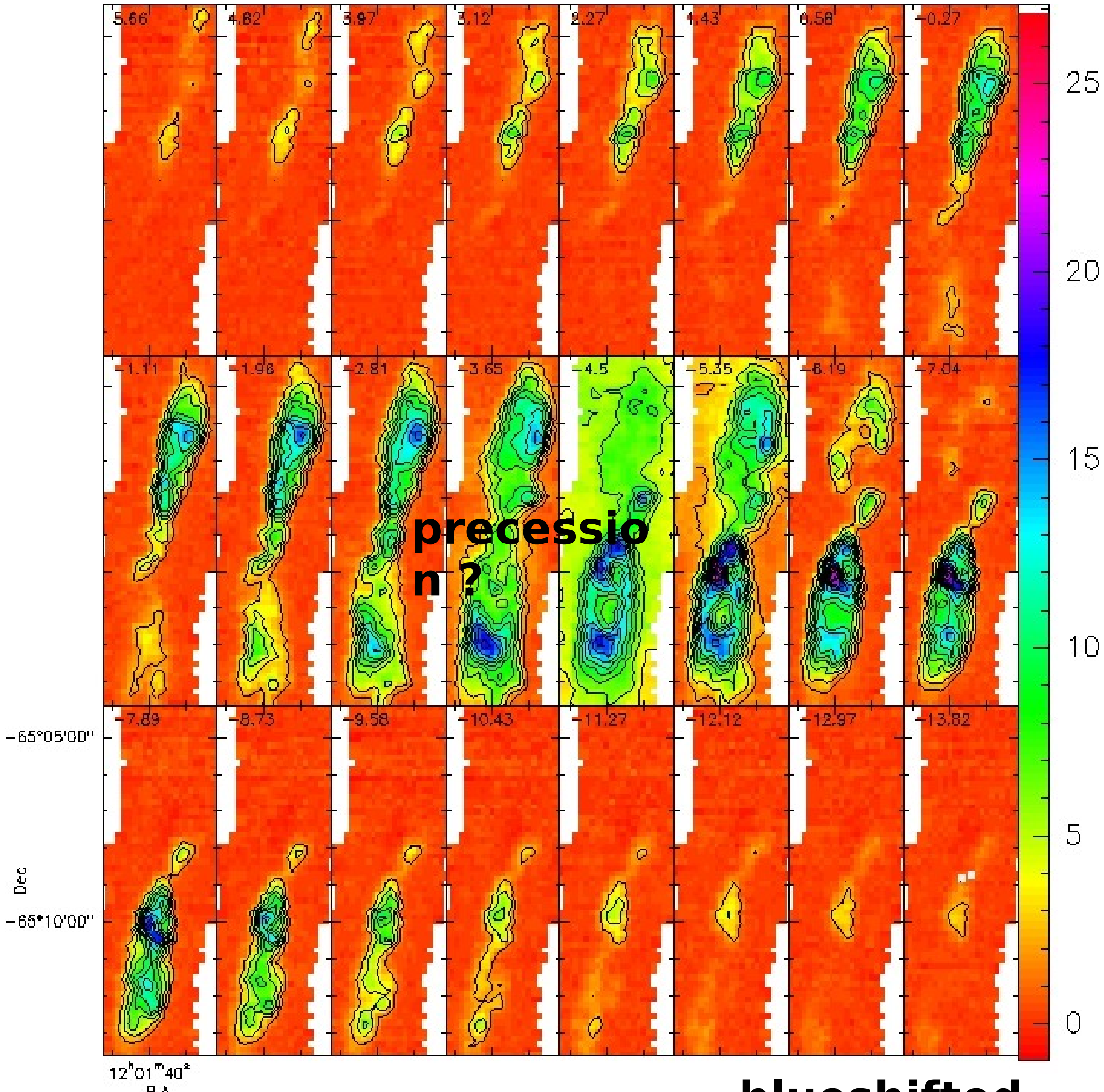

blueshifted

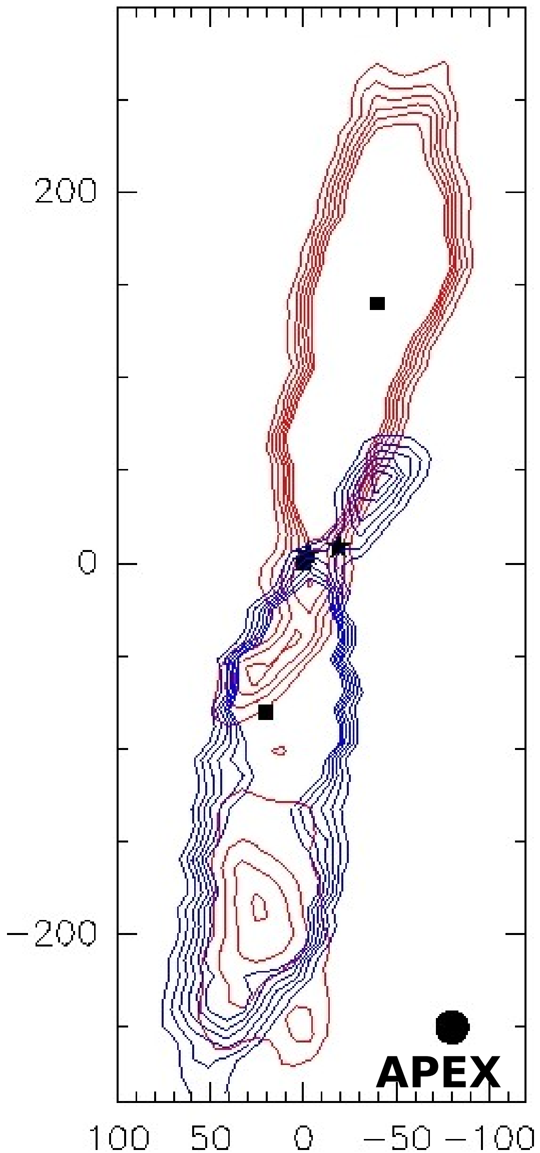

imaging of the second outflow !

Velocity structure traced by CO

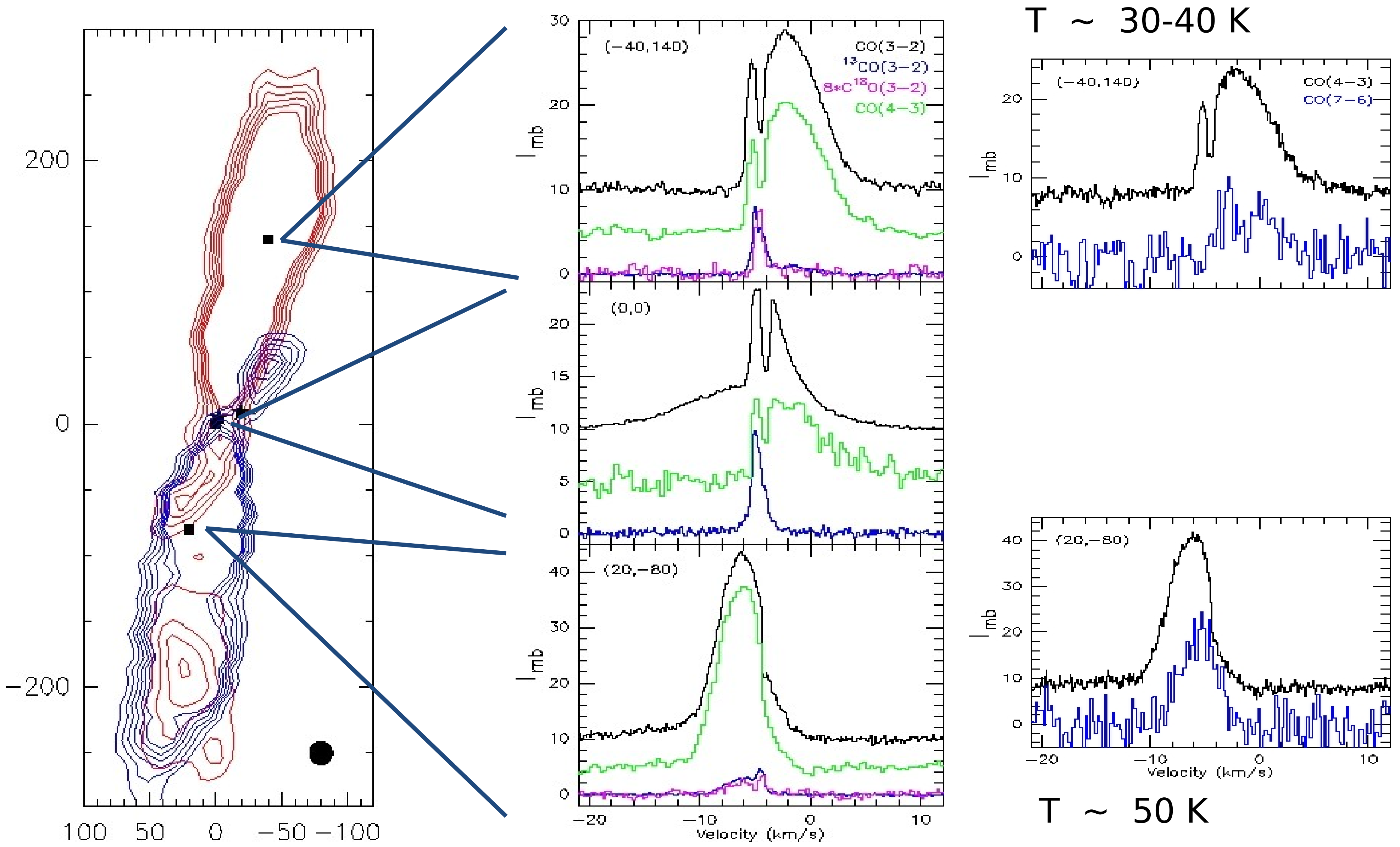

Physical diagnostic using methanol

preshock gas ?

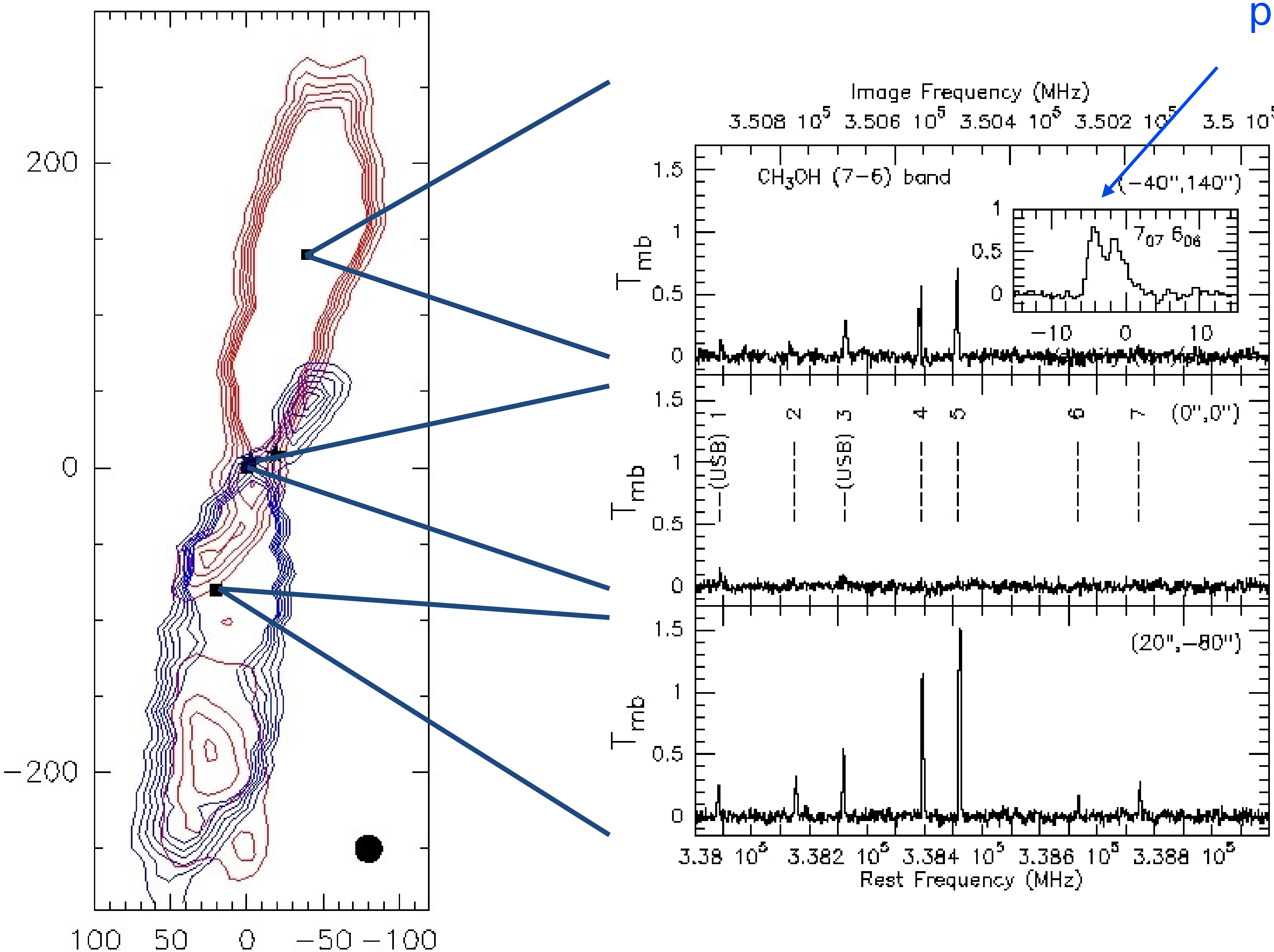

T ~ 20-30 K

n ~ 10^5 cm^{-3}

T ~ 10K

30 <T< 50 K

10^5 <n< 3.10^5

IRAS 19410: how high resolution changes the picture

from 2 to 6 cores; from 2 to 9 flows

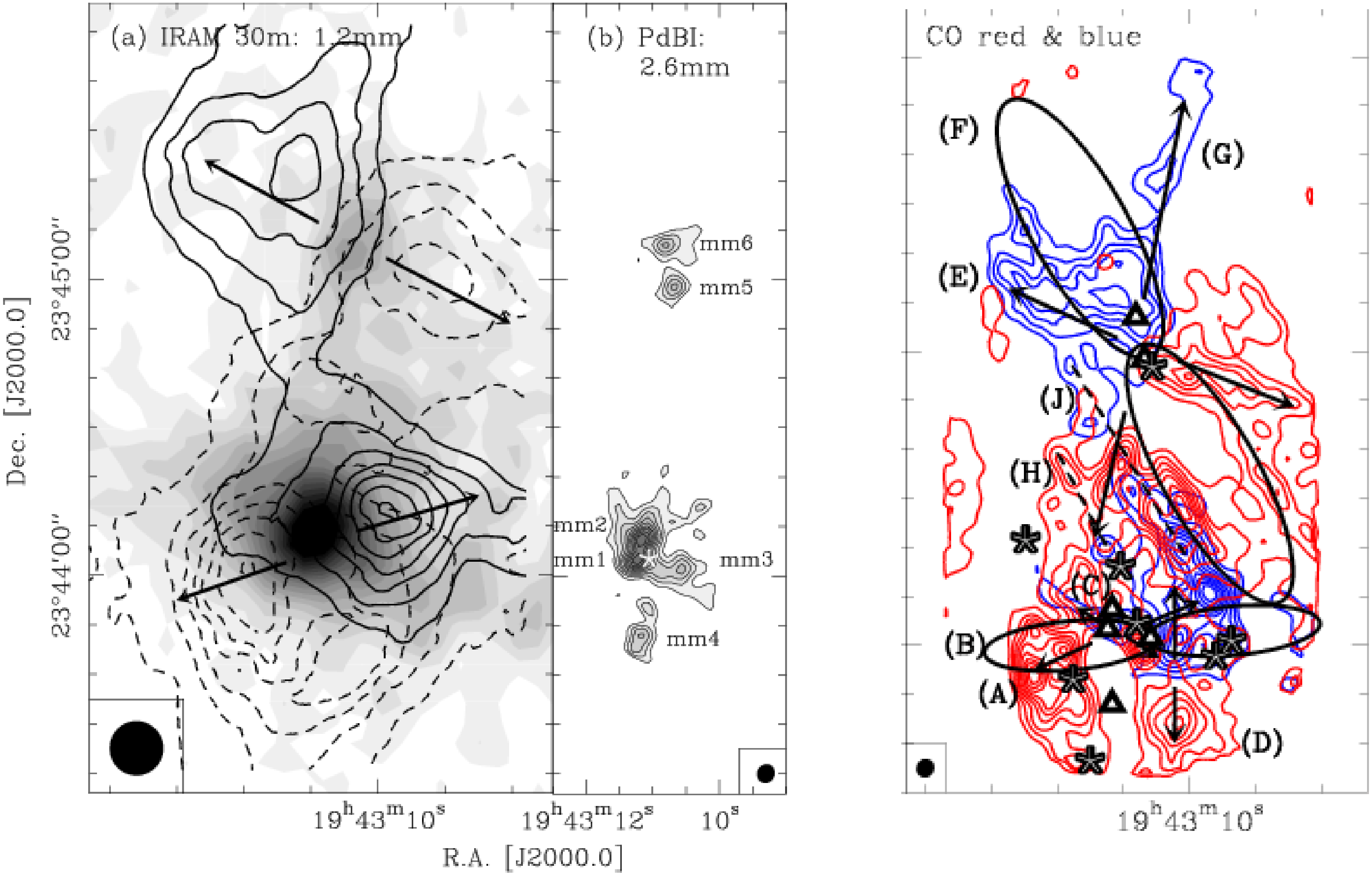

Molecular Outflows

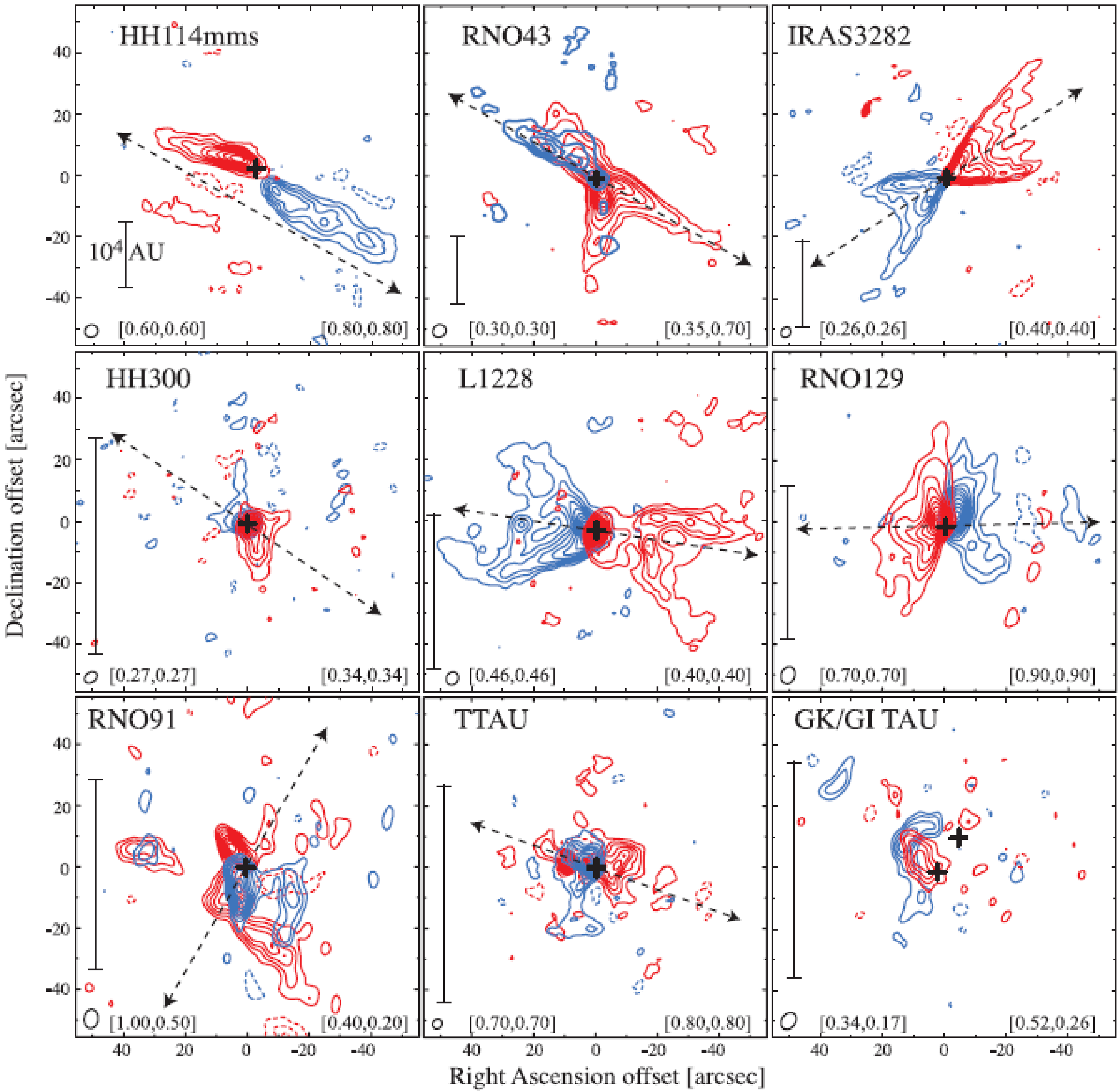

Numerous out-flows show a relatively wide angle

Jets and Outflows

- Most dramatic phenomenon as evidence of star formation.
- Common phenomenon from proto-brown dwarfs (with 0.03 $M_\odot$) up to very massive stars (10 $M_\odot$)
- For low mass stars, flows of younger stars are
  - faster
  - more highly collimated
- Influence the surrounding material both mechanically and thermally.
- Contrary to the disks, jets and outflows were not predicted by rotating infall theory
- Jets of AGNs are probably similar phenomena

Jets and Outflows

Questions:

- Launching process
- Contribution to angular momentum removal
- Relation between jet and outflows
- Confinement

Basic picture

Jet:
• extremely collimated, high velocity flow
• away from center of collapse, perpendicular to disk
• evolution complementary to disk evolution

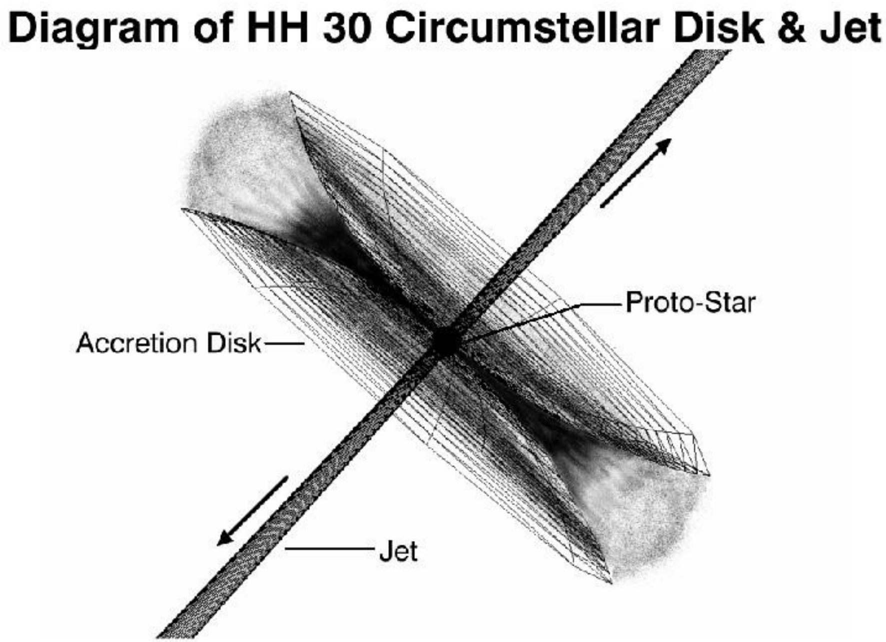

Basic picture

Combination of jet and molecular outflow:

- Multiple velocity components

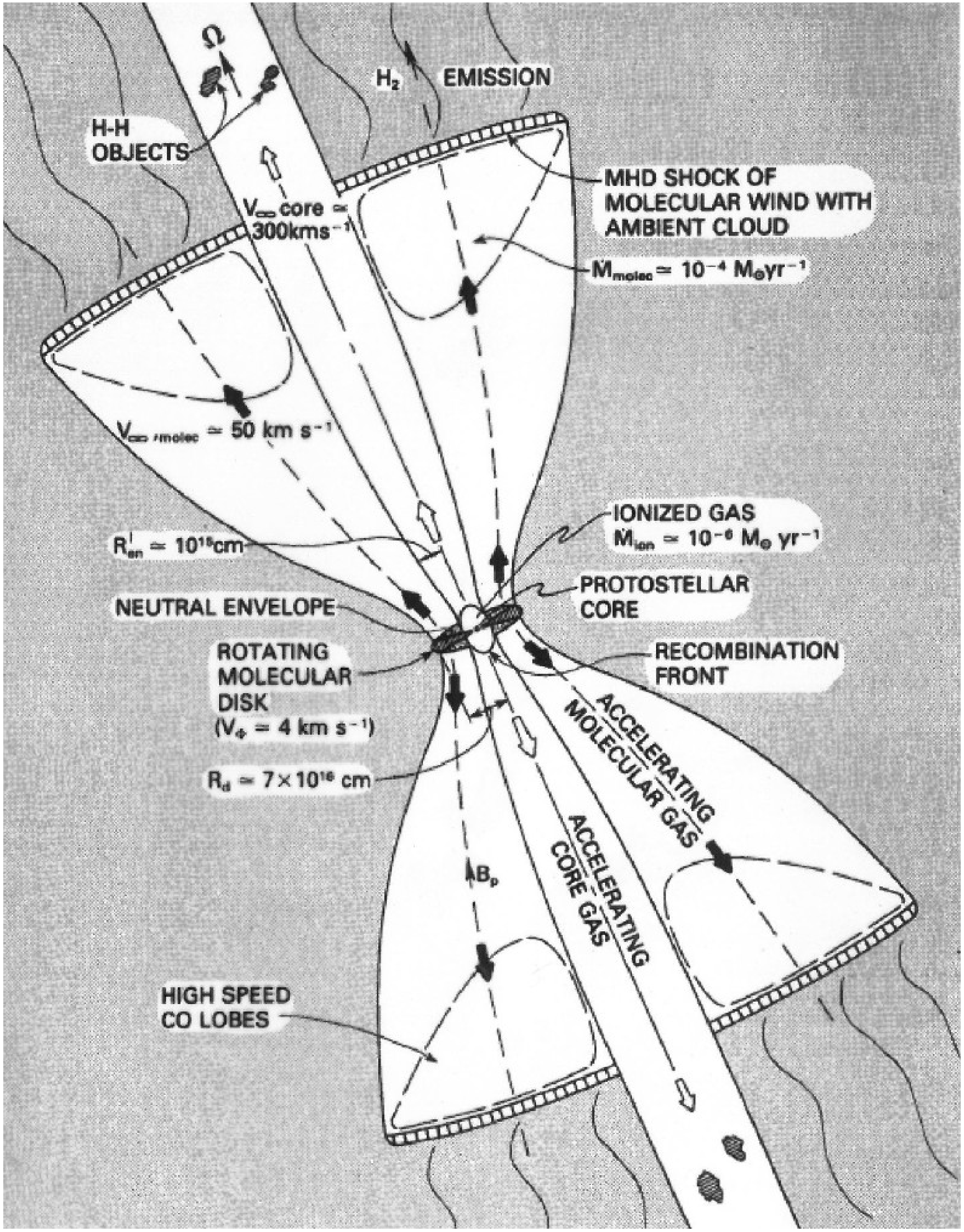

Observations

Line shape tracing wind:

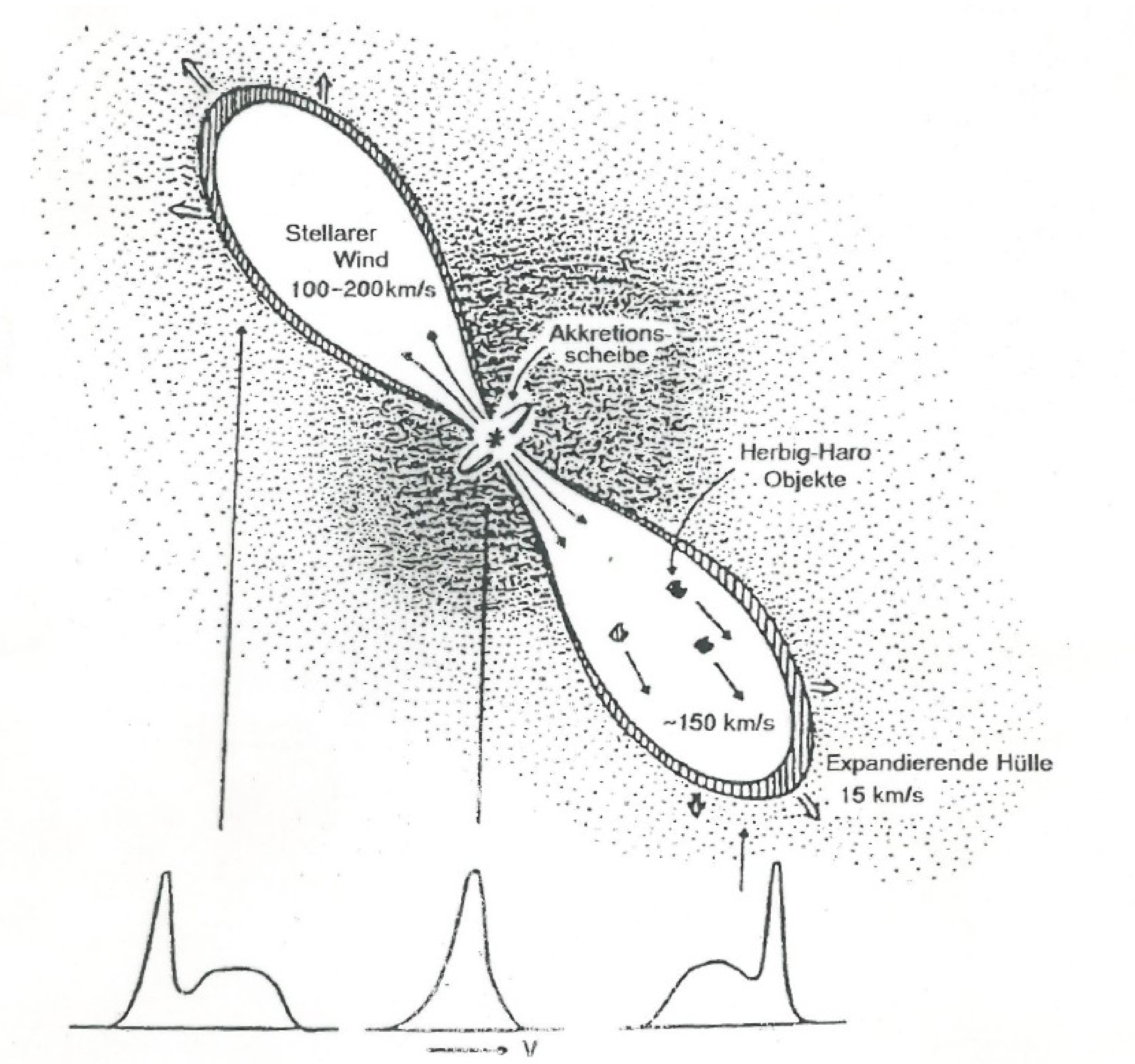

Abbildung 4.6: Schematisches Modell eines jungen Sterns mit bipolarem Ausfluß. Unten sind die CO-Spektren mit den entsprechenden Linienverschiebungen, bedingt durch die Neigung des Jets zur Sichtlinie, für drei unterschiedliche Bereiche des Objektes angegeben. Die linke und rechte Linie hat die Form eines P-Cygni-Profils.

Geometry and confinement

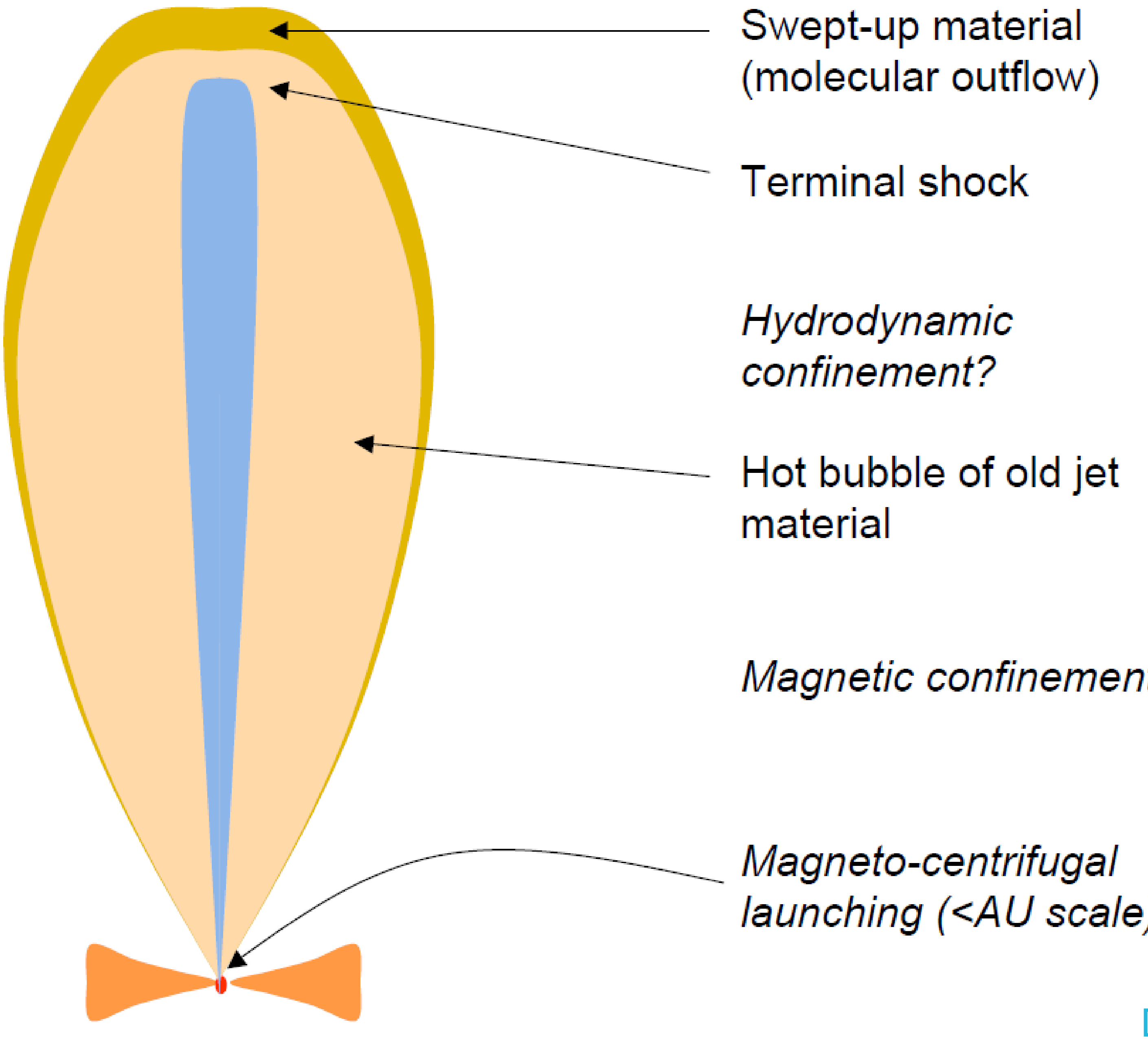

Dullemond (2010)

Magnetic field winding - confinement

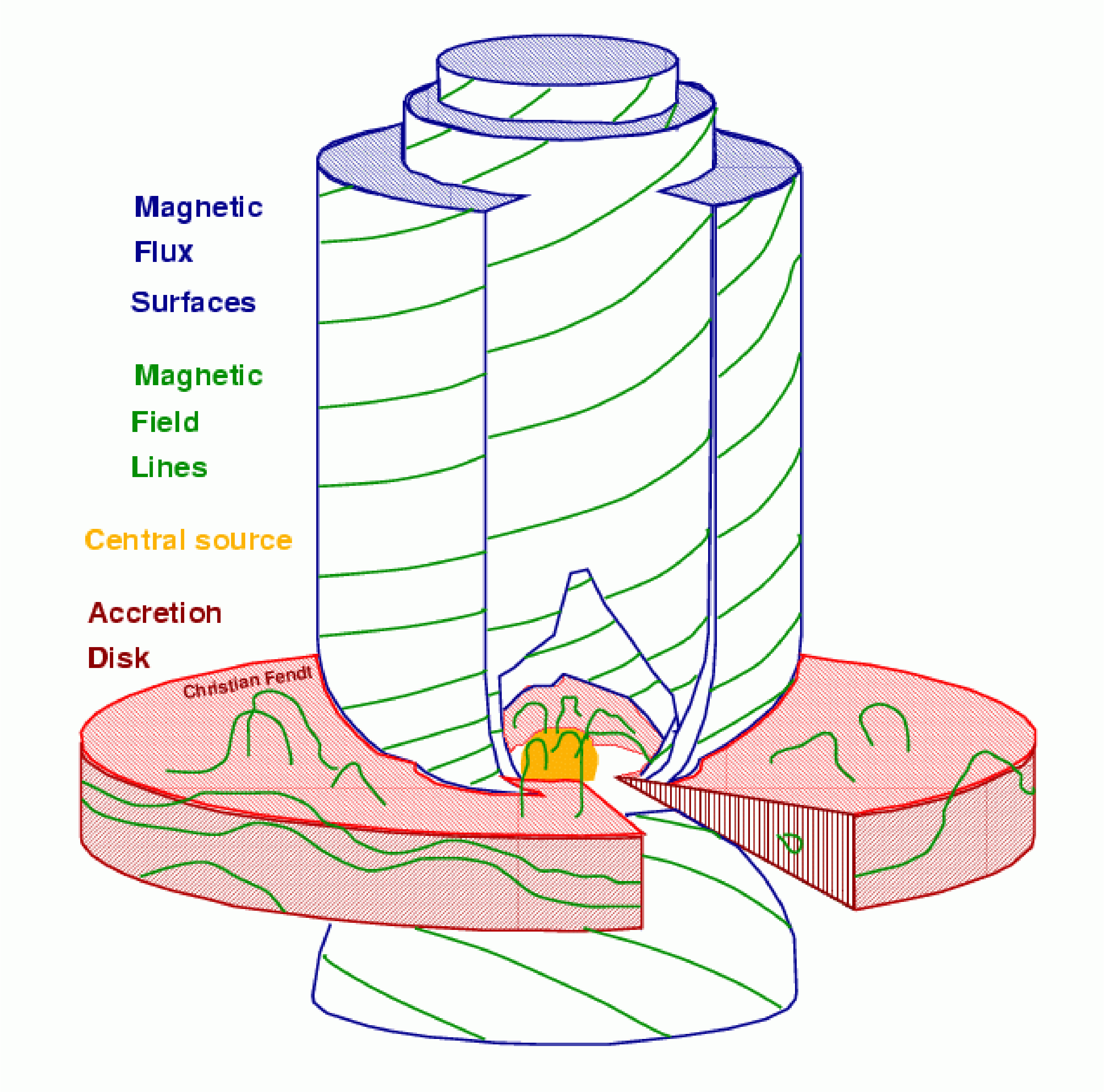

C. Fendt

Magnetic field winding - confinement

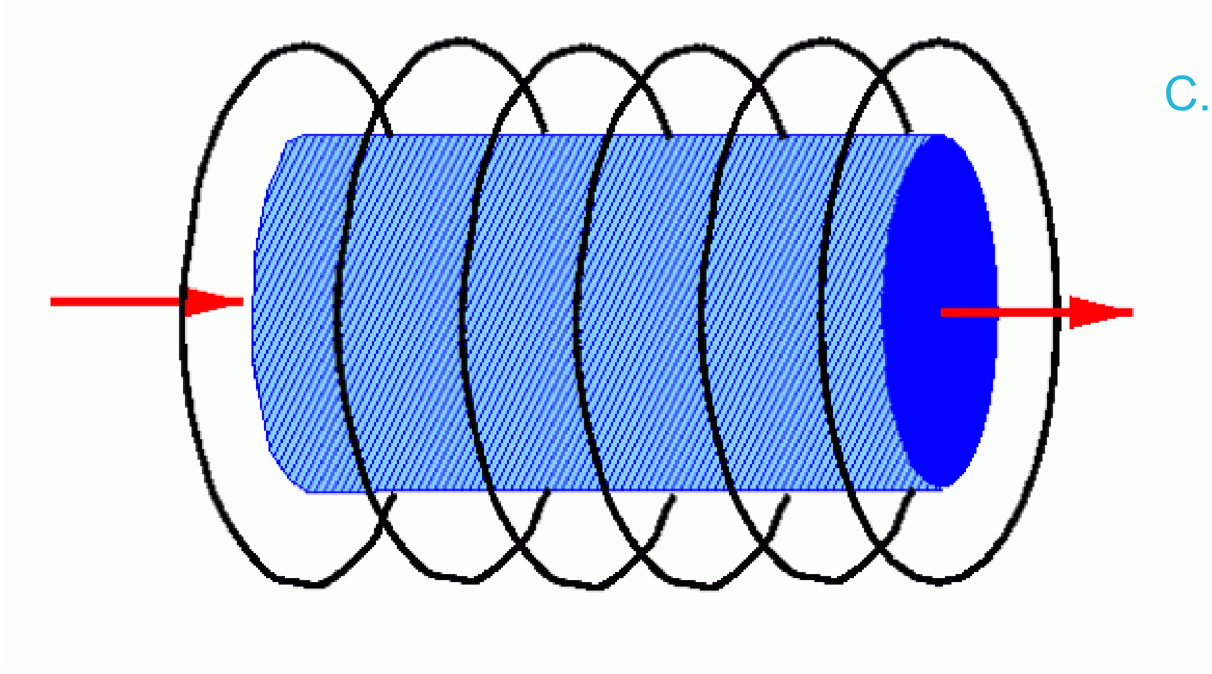

C. Fendt

$$\vec{j} = \frac{c}{4\pi} \nabla \times \vec{B}$$

$$\vec{f} = \frac{1}{c} \vec{j} \times \vec{B}$$

- Right-hand rule:
  force points inwards

Hydrodynamic confinement of jets

- Jets are surrounded by cocoon of pressurized gas
  - Cocoon partly made of old jet material, partly by swept up material from the environment
  - Jet material moves *supersonically*

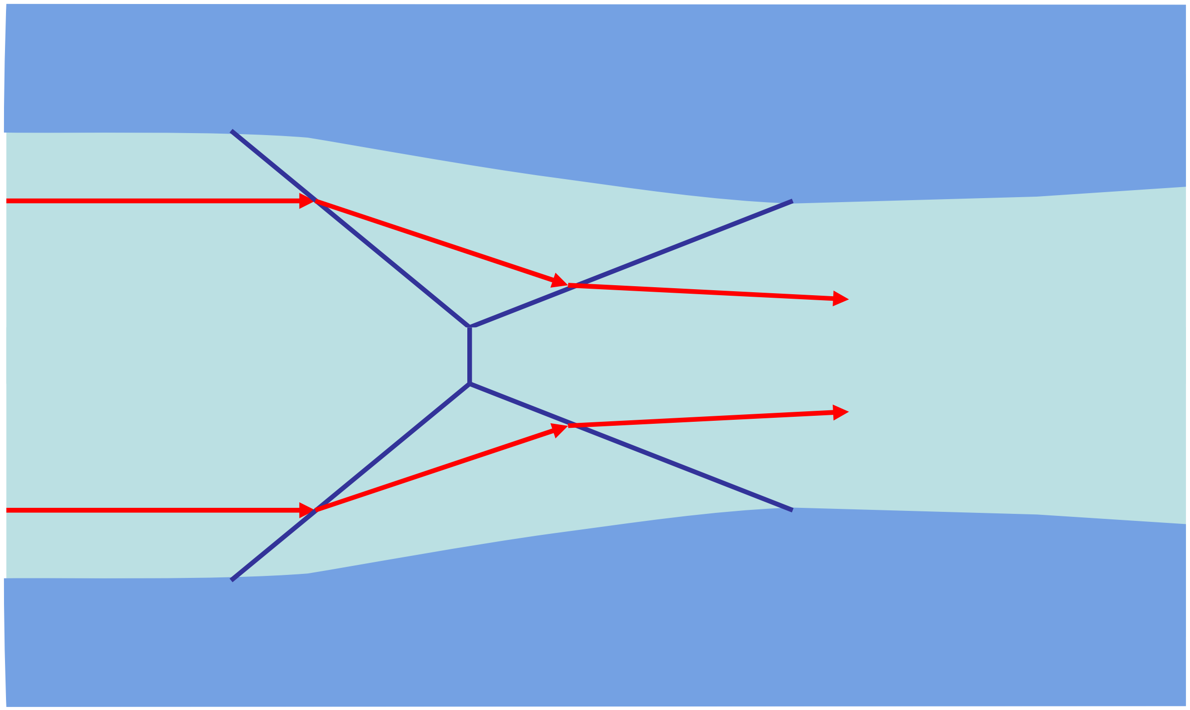

- Shock only reduces the velocity compon-ent perpendicular to shock front. Therefore obliquely shocked gas is deflected toward the shock plane.

Hydrodynamic confinement in jet:

Dryden Flight Research Center EC93-03092-7 Photographed 1994
SR-71 Ship #1

Hydrodynamic confinement of jets

- Head of jet ('hot spot') drills through ISM
- Shocks seen as knots (Herbig-Haro objects)

Observed knot movement (HH30)

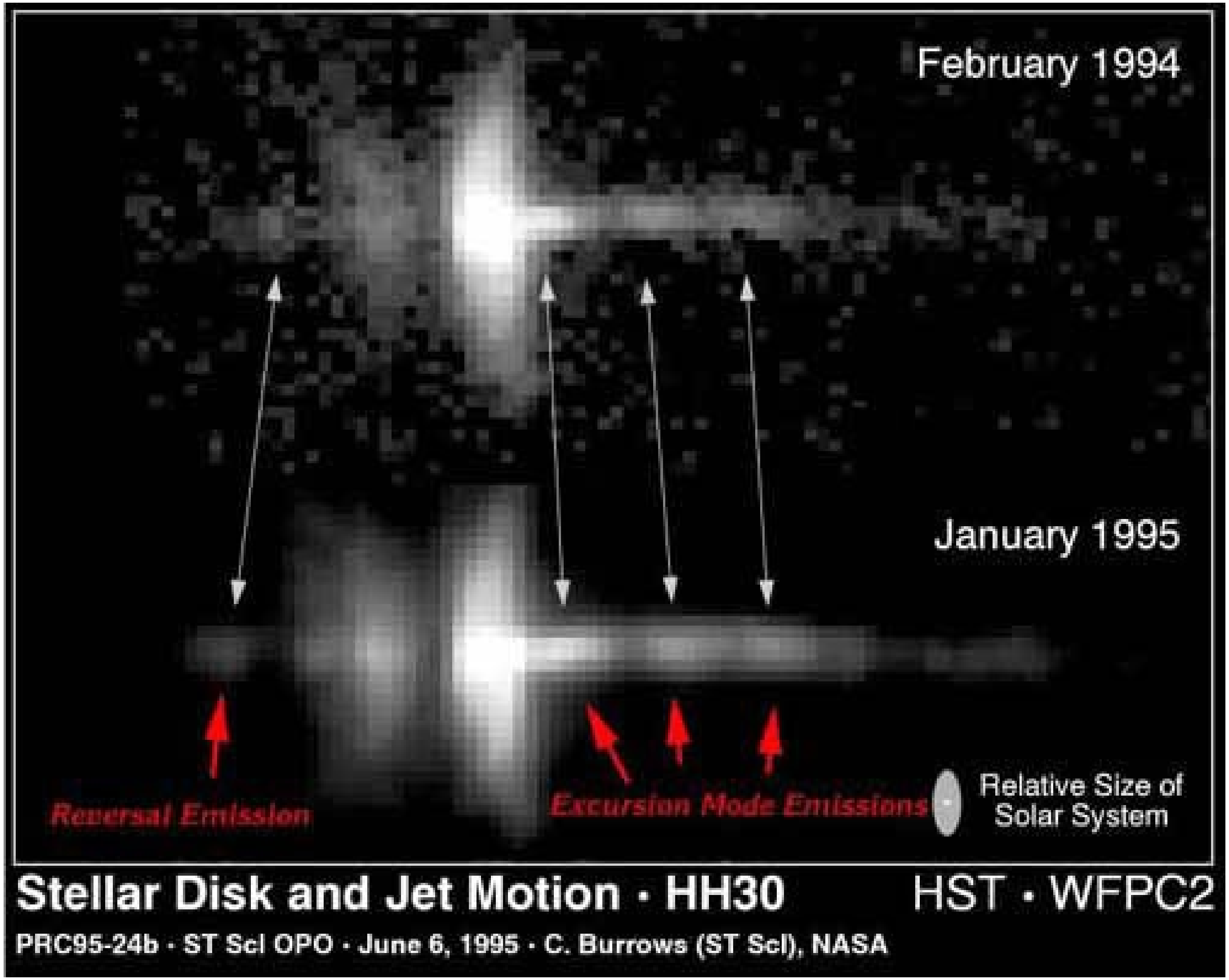

Molecular flows: entrainment

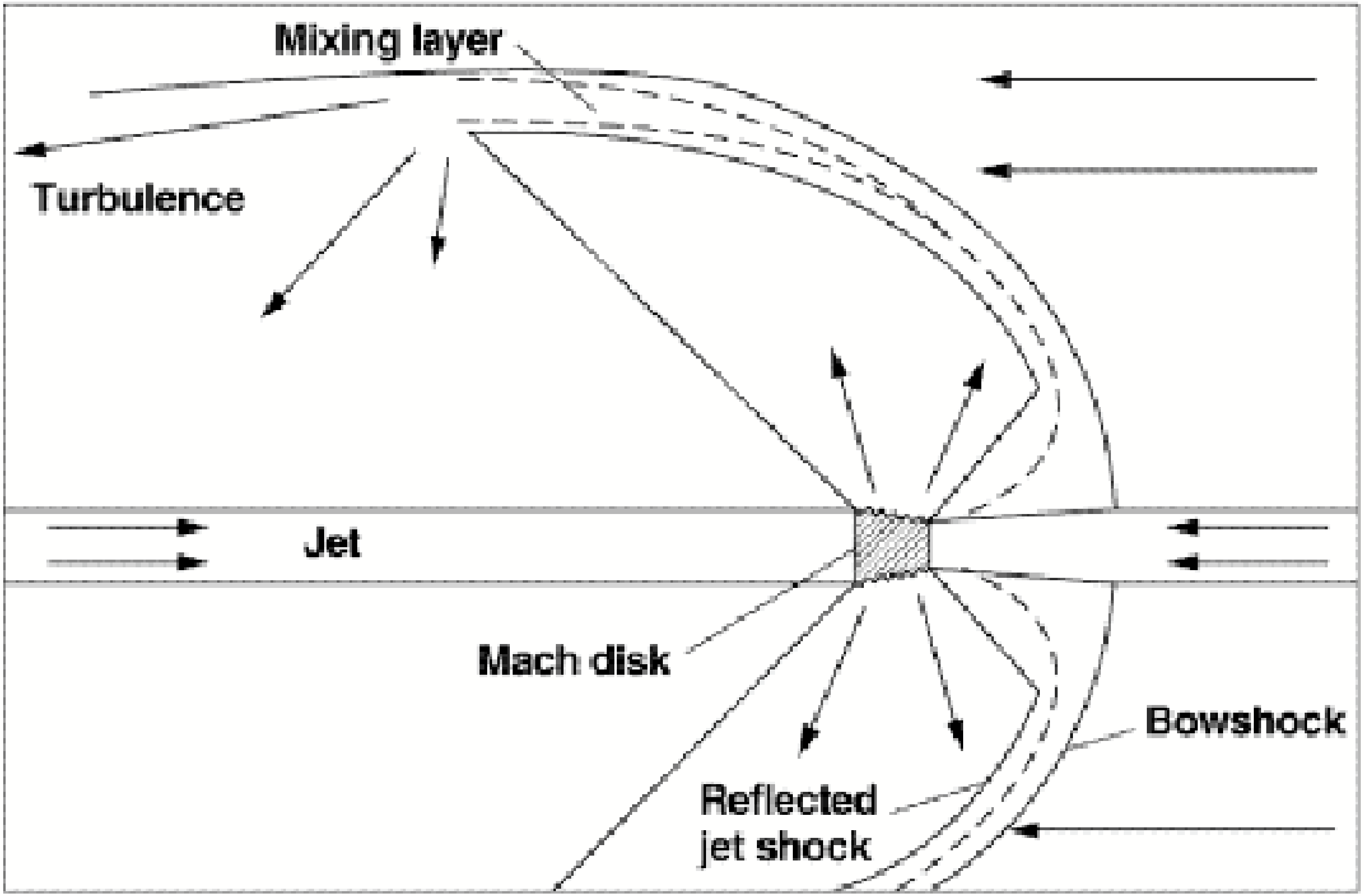

Molecular flows: observation

Velocity nesting: gas with higher velocity is more collimated, lower velocity outflow is more extended

Position-velocity diagrams:

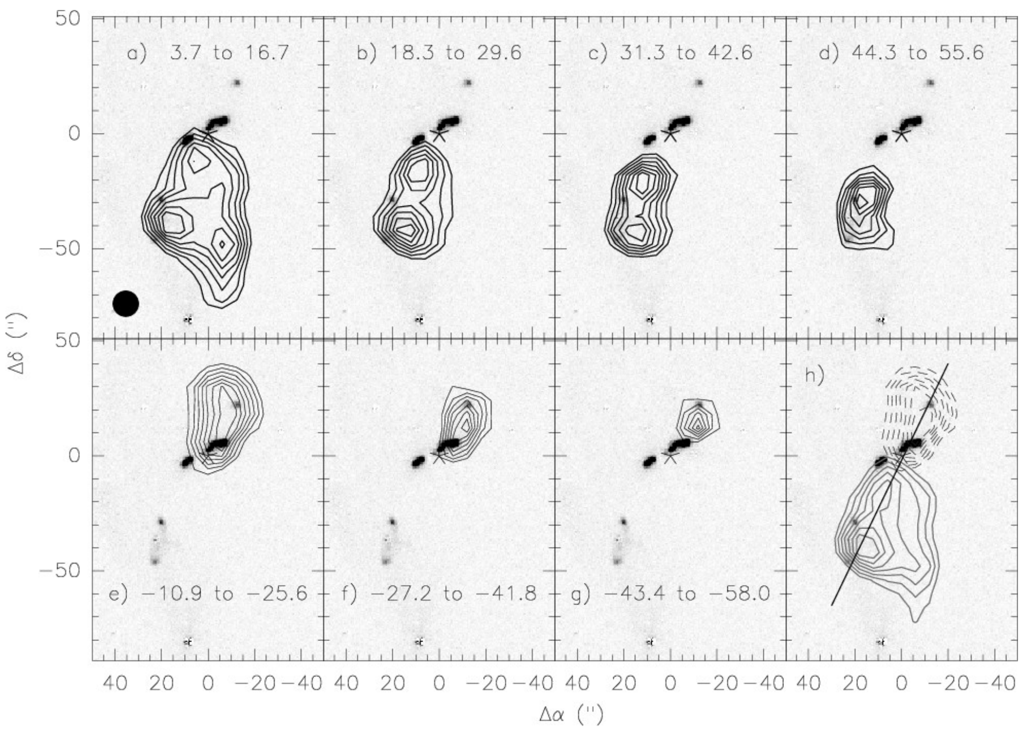

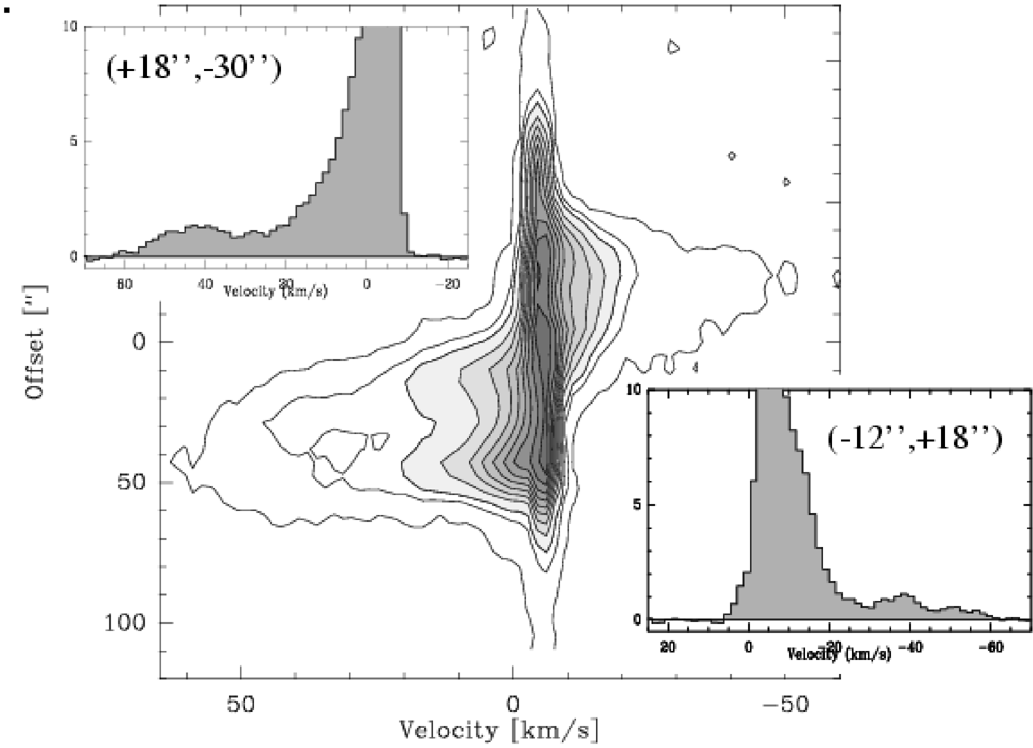

The extremely high-velocity molecular outflow in IRAS 20126+4104 (Lebrón et al. 2006)

Jet simulations

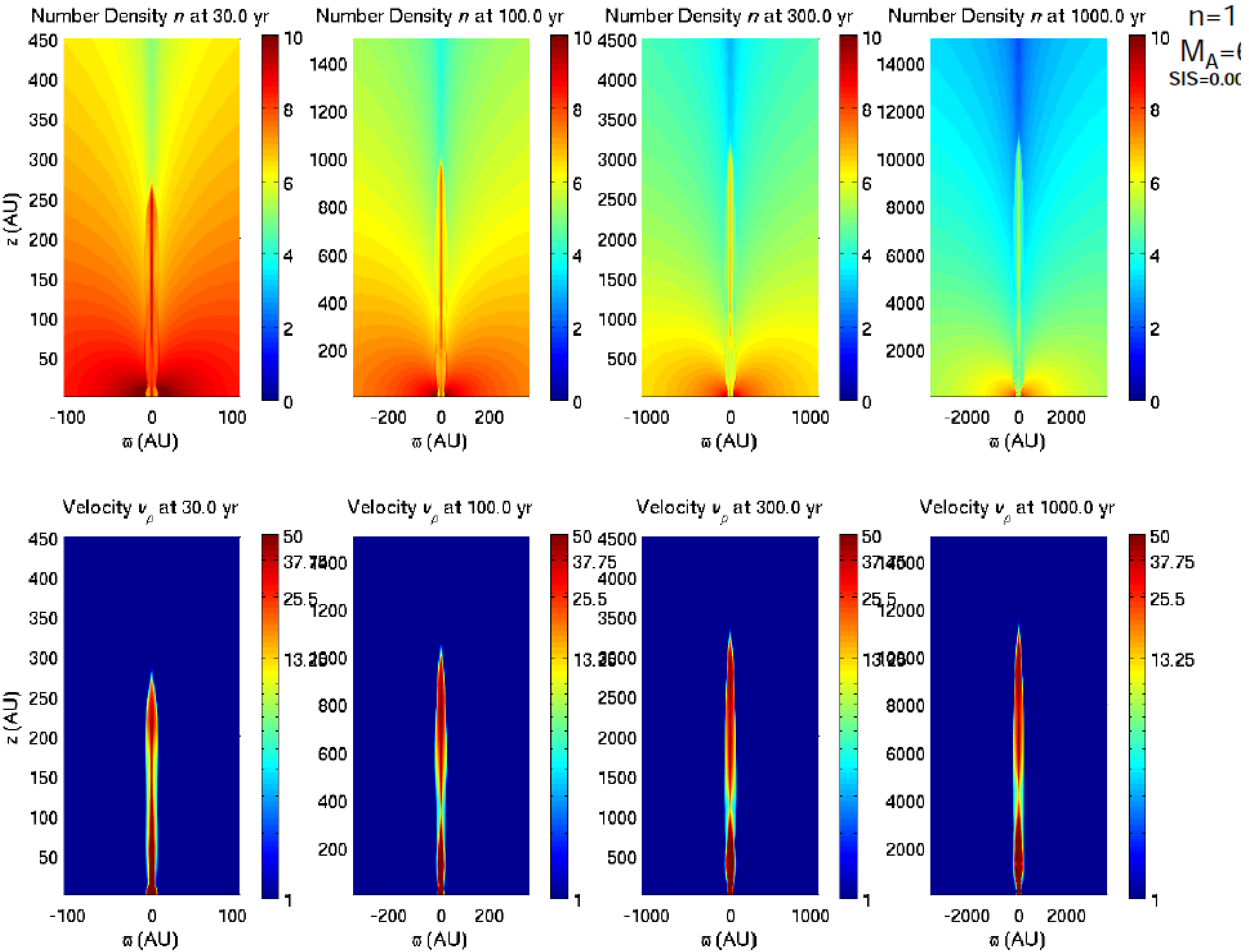

Number Density n at 30.0 yr
Number Density n at 100.0 yr
Number Density n at 300.0 yr
Number Density n at 1000.0 yr
n=1
SIS=0.00
z (AU)
ϖ (AU)
Velocity v_ρ at 30.0 yr
Velocity v_ρ at 100.0 yr
Velocity v_ρ at 300.0 yr
Velocity v_ρ at 1000.0 yr
z (AU)
ϖ (AU)
50
37.75
25.5
13.25

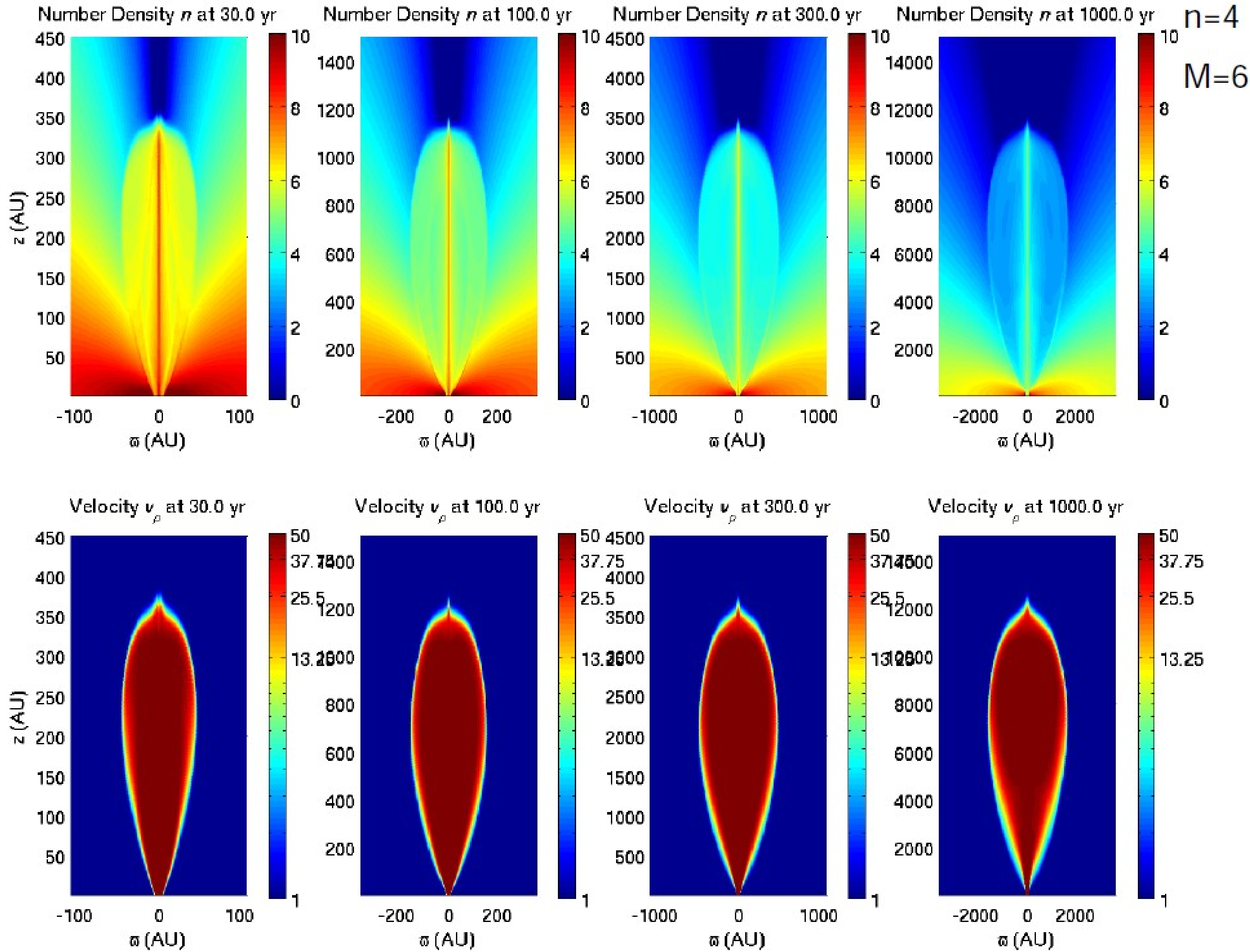

n=4
M=6
Number Density n at 30.0 yr
Number Density n at 100.0 yr
Number Density n at 300.0 yr
Number Density n at 1000.0 yr
Velocity v_ρ at 30.0 yr
Velocity v_ρ at 100.0 yr
Velocity v_ρ at 300.0 yr
Velocity v_ρ at 1000.0 yr
z (AU)
ϖ (AU)

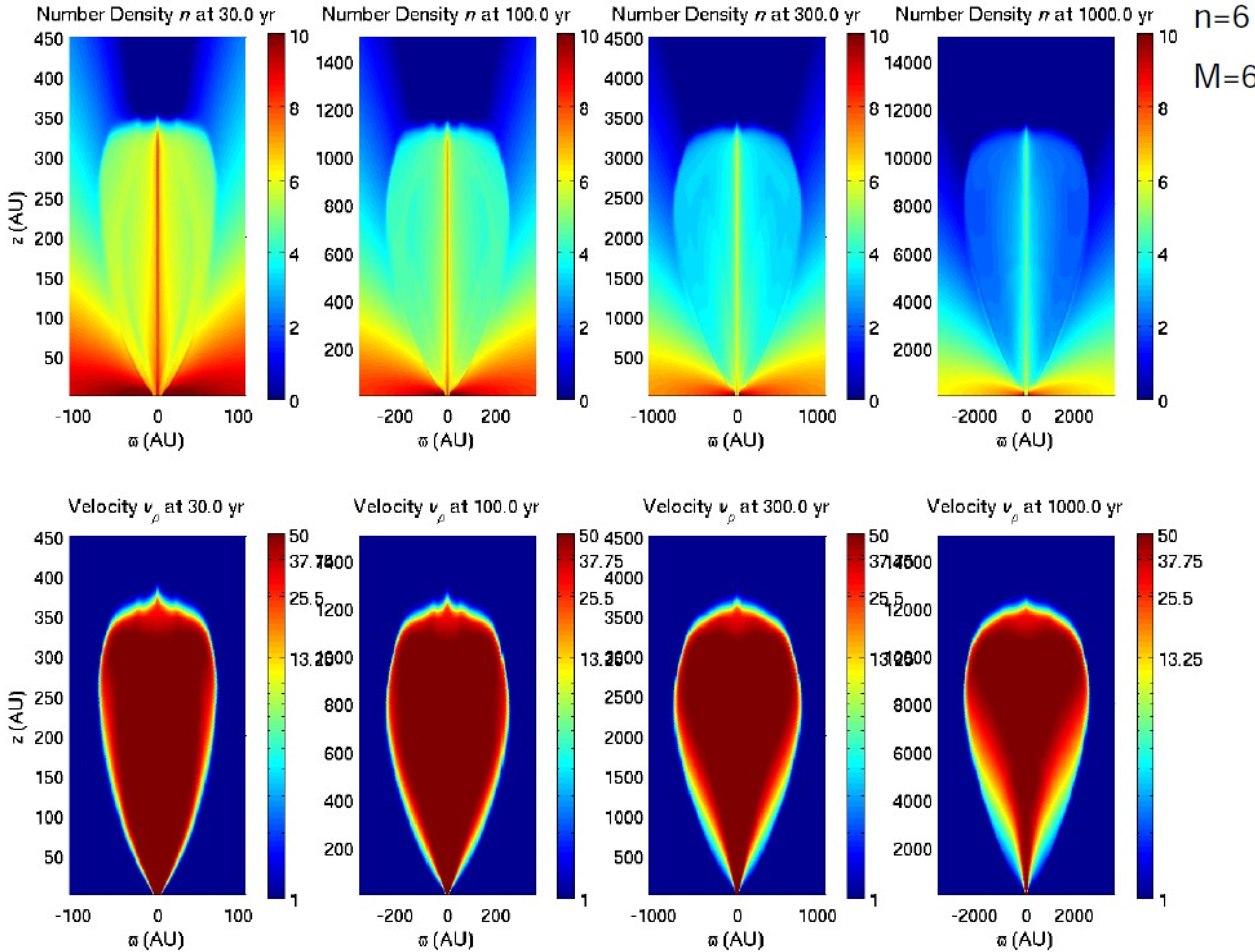

Number Density n at 30.0 yr
Number Density n at 100.0 yr
Number Density n at 300.0 yr
Number Density n at 1000.0 yr
n=6
M=6
Velocity v_ρ at 30.0 yr
Velocity v_ρ at 100.0 yr
Velocity v_ρ at 300.0 yr
Velocity v_ρ at 1000.0 yr
z (AU)
ϖ (AU)
0
2
4
6
8
10
1
13.25
25.5
37.75
50

n=2

M=60

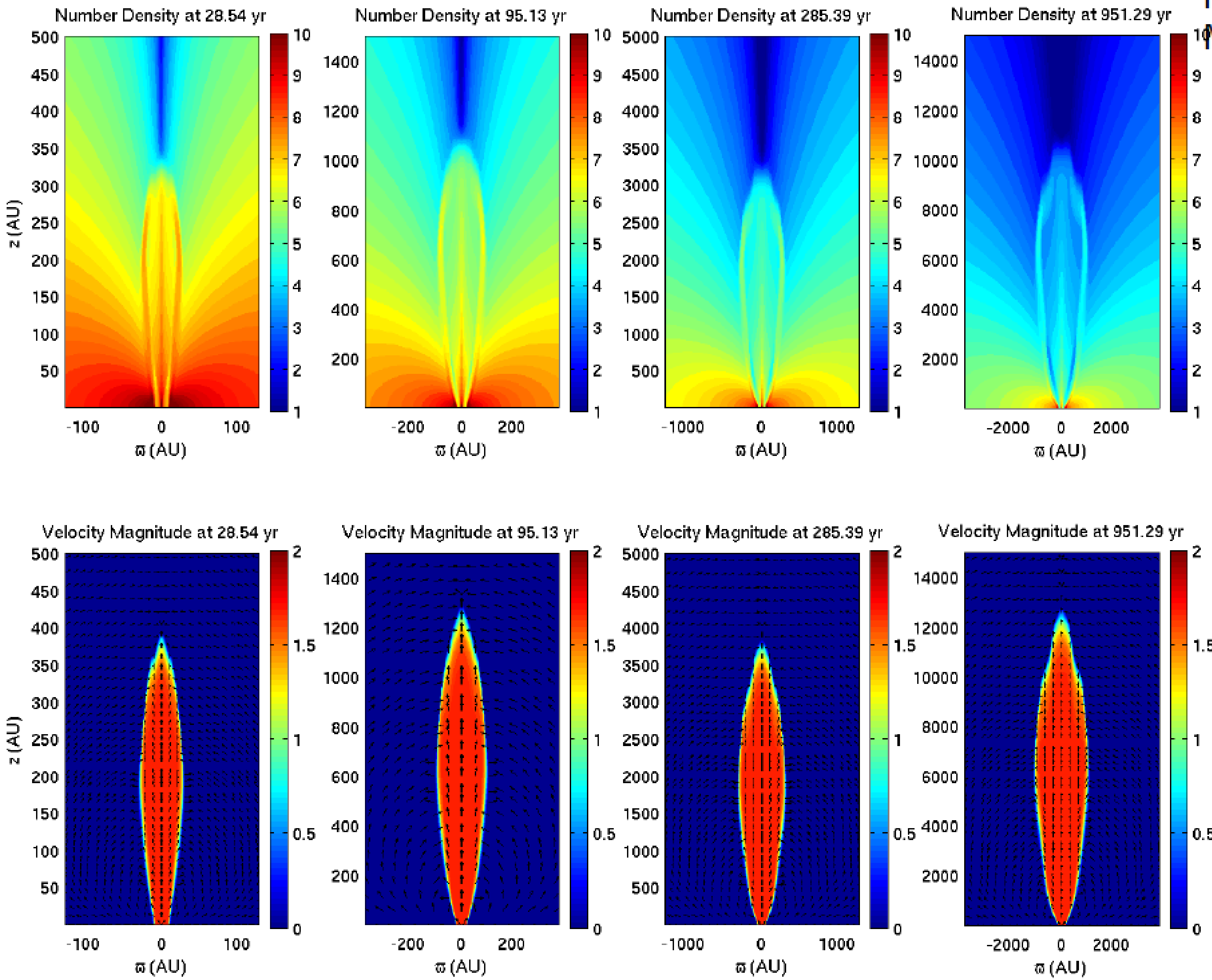

Shang et al (2005)

n=6
M=6(

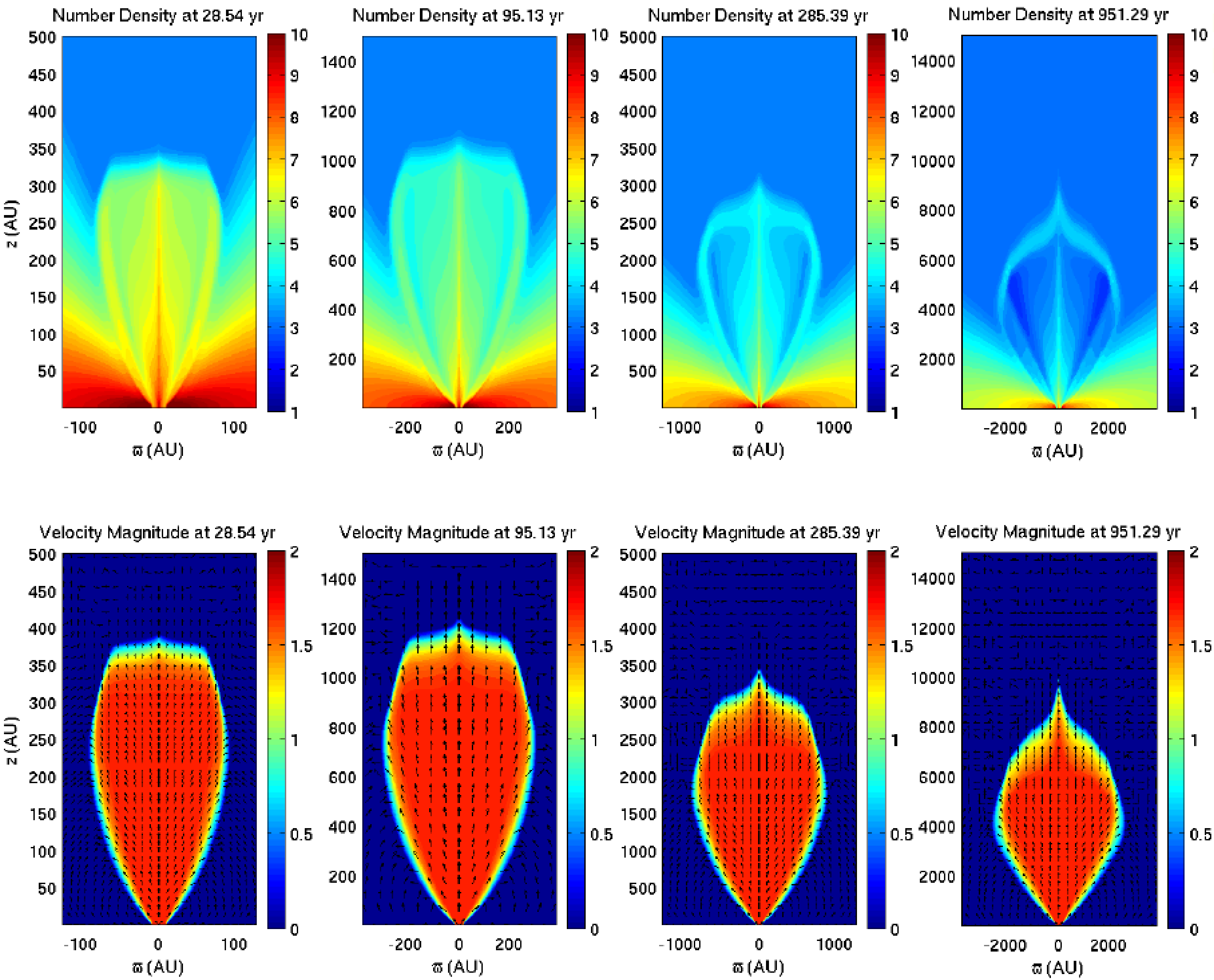

Shang et al (2005)

Launching processes?

Correlation between mass outflow and accretion:

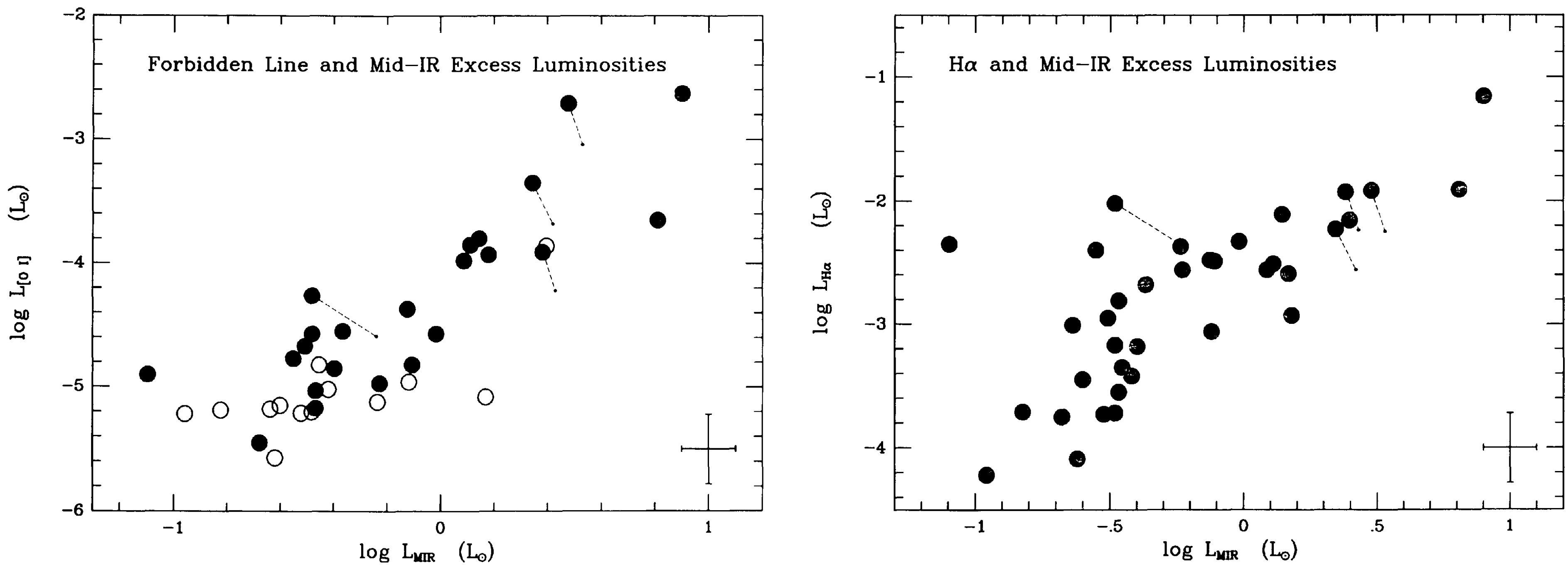

FIG. 5a FIG. 5b

FIG. 5.—(*a*) Relationship between the dereddened [O I] λ6300 luminosity $L_{[\mathrm{O\,I}]}$ and the mid-IR excess luminosity L_{MIR} for the 36 stars in our sample (symbols as in Fig. 4). (*b*) Relationship between the dereddened Hα luminosity $L_{\mathrm{H}\alpha}$ and the mid-IR luminosity excess L_{MIR} for the 36 TTS in our sample. In both of these plots, the two quantities are well correlated over two orders of magnitude (the only exception is GM Aur, a star with strong [O I] and Hα emission but small mid-IR excess. However, if this is a CTTS with a nearly edge-on disk, it will not violate the correlations). Note that uncertainties in A_V tend to increase the scatter in these plots.

Cabrit et al. 1990

- Jet masses traced by excited lines of ionized gas
- Accretion in protostellar phase measured by total luminosity (up to 10^{-3} $M_{\odot}$/yr)

Launching processes?

Correlation between mass outflow and accretion:

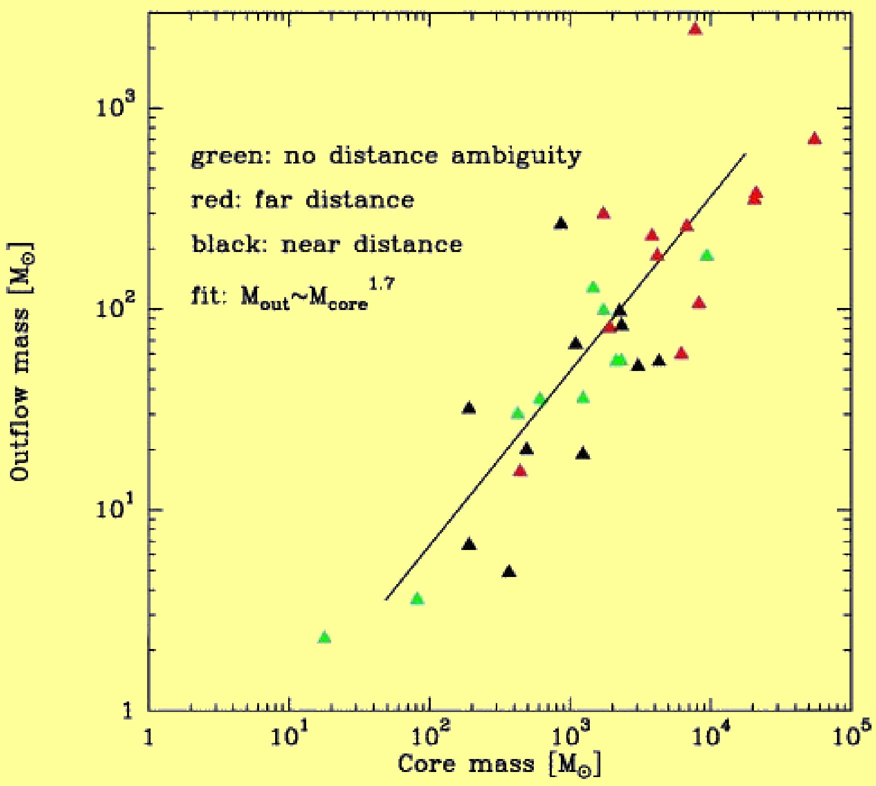

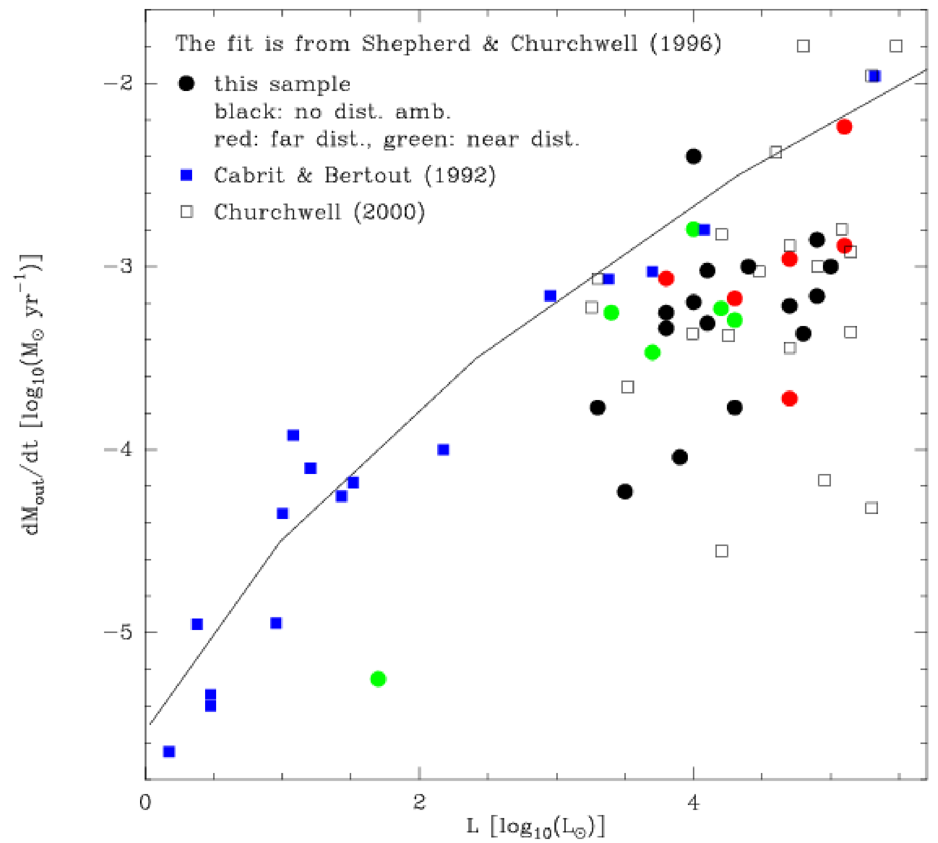

Molecular outflow mass

Outflow rate

→ close relation between accretion and outflow generation

→ favors some MHD jet launching mechanism

Jet formation

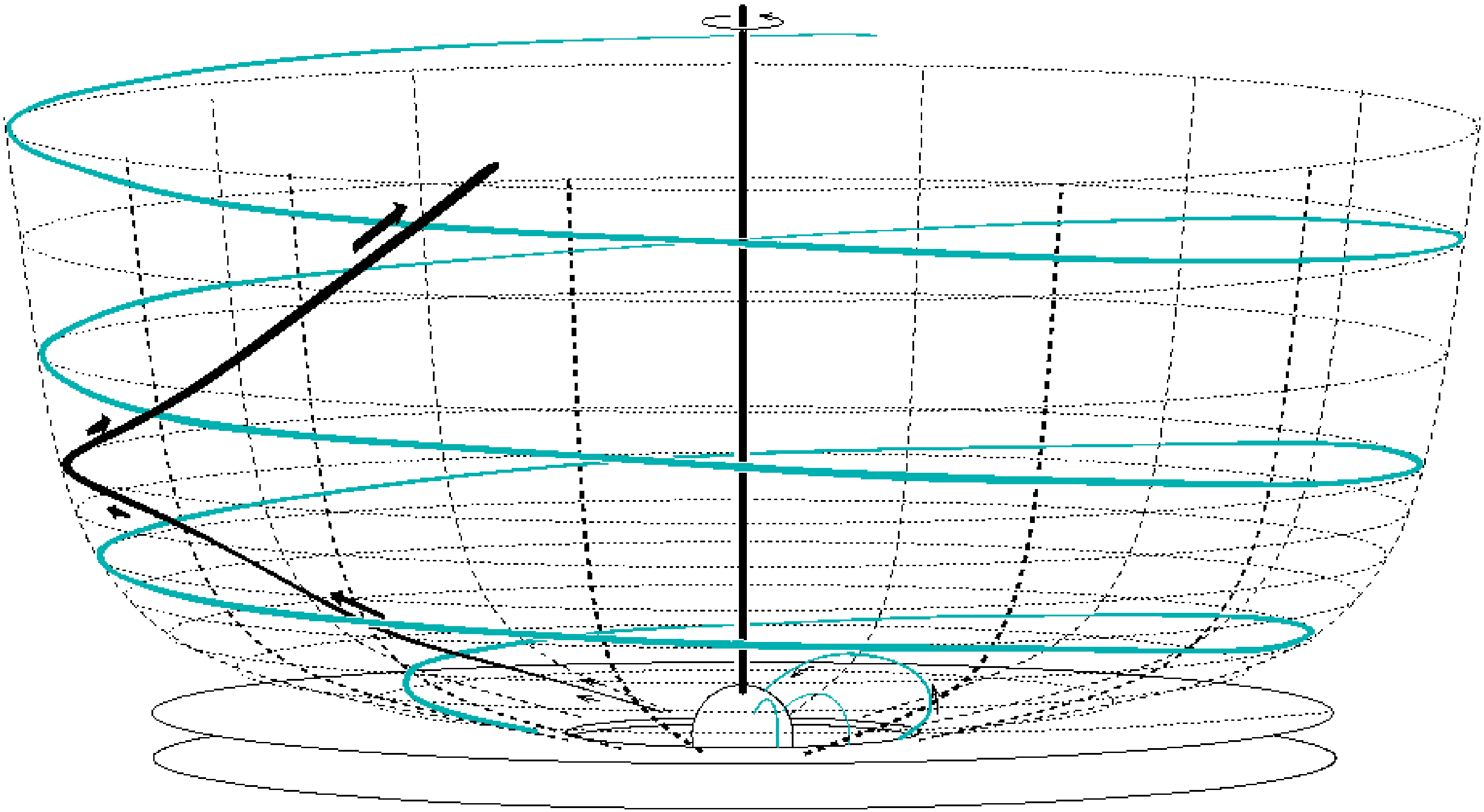

Two competing theories:

X-wind model ↔ Disk-wind model

Magnetospheric accretion

Inner disk boundary: $\Omega_{\text{disk}} \approx \Omega_{\text{star}}$

Corotation radius $r_{co} = \left(\frac{GM}{\Omega_{star}^2} \right)^{1/3}$

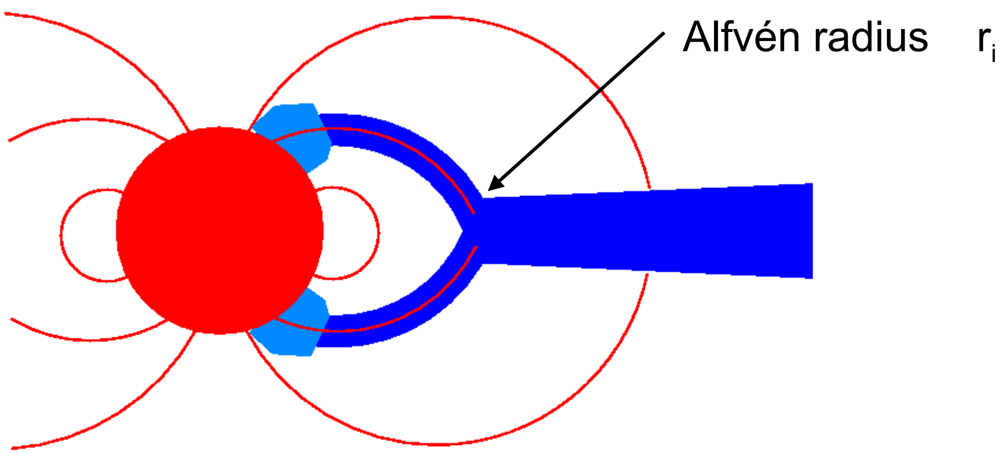

- Magnetic coupling between disk and star
- Accretion along the field lines

Königl (1991)

- Gas is loaded onto magnetic field lines (disk is destroyed) where magnetic pressure = dynamic pressure.

“X”-wind

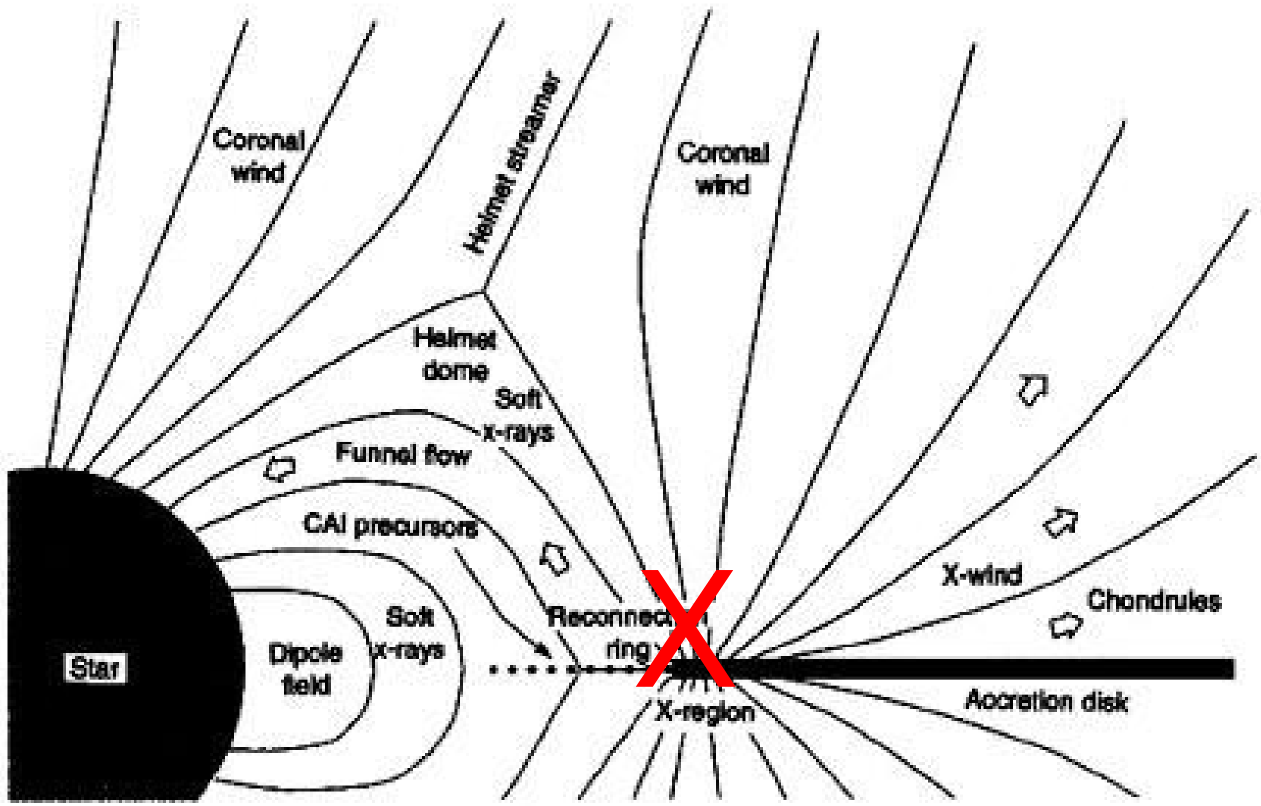

In the X-wind model the magnetic field of a young star interacts with the magnetic field of the circumstellar disk to produce a gap between the star and disk. As gas spirals inward through the disk, it divides at the inner disk edge (the X-region) into two streams. A high angular momentum stream is flung away along the rotating magnetic field lines of the disk (the X-wind); the low angular momentum stream falls onto the star and helps build its mass.

X-wind

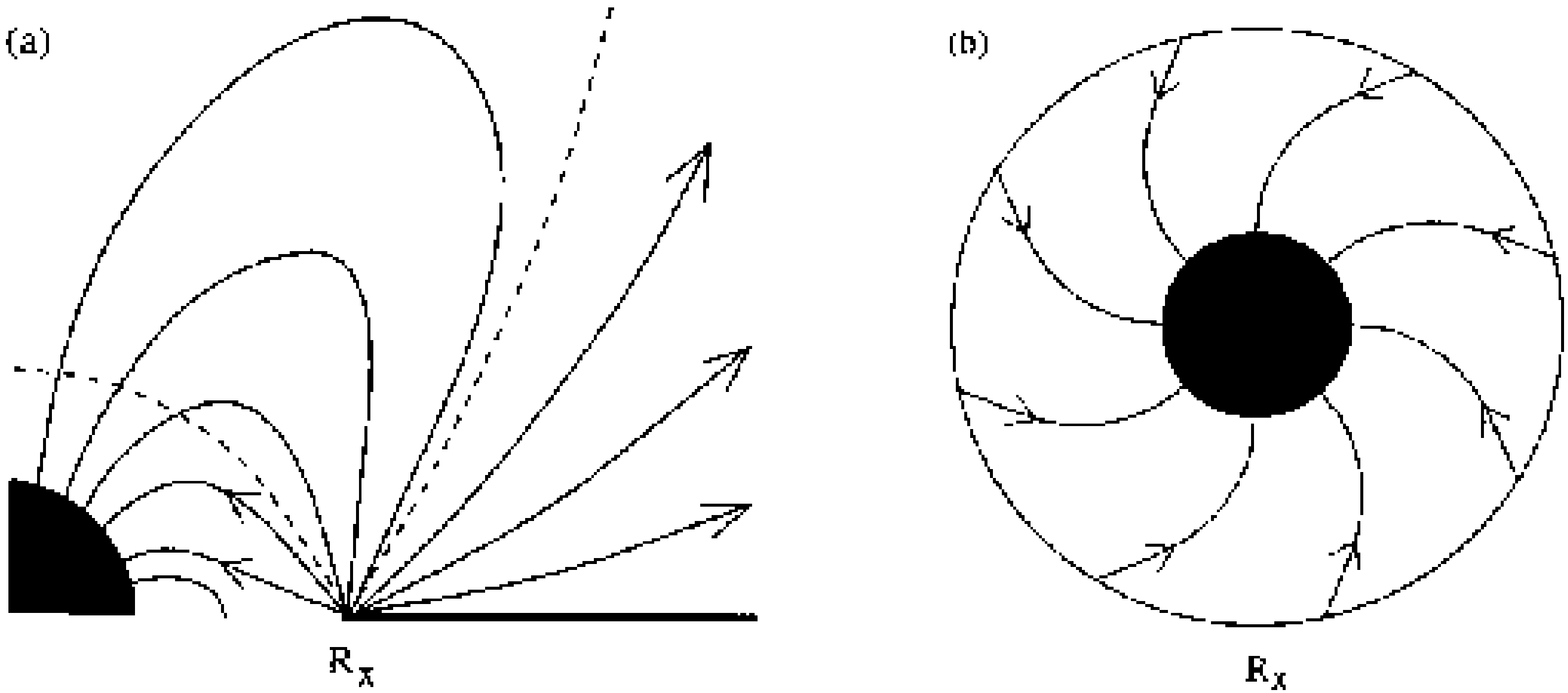

Figure 13 Schematic views of the (*a*) meridional plane and (*b*) equatorial plane of the configuration modeled by Shu et al (1994a,b) for the origin of bipolar outflows. The circumstellar disk is truncated at a distance R_X from the star. Both energetic outflows and funnel flows emerge from the disk truncation region. Gas accreting from the disk onto the star in a funnel flow drags the stellar field into a trailing spiral pattern. (From Najita 1995.)

X-wind simulation

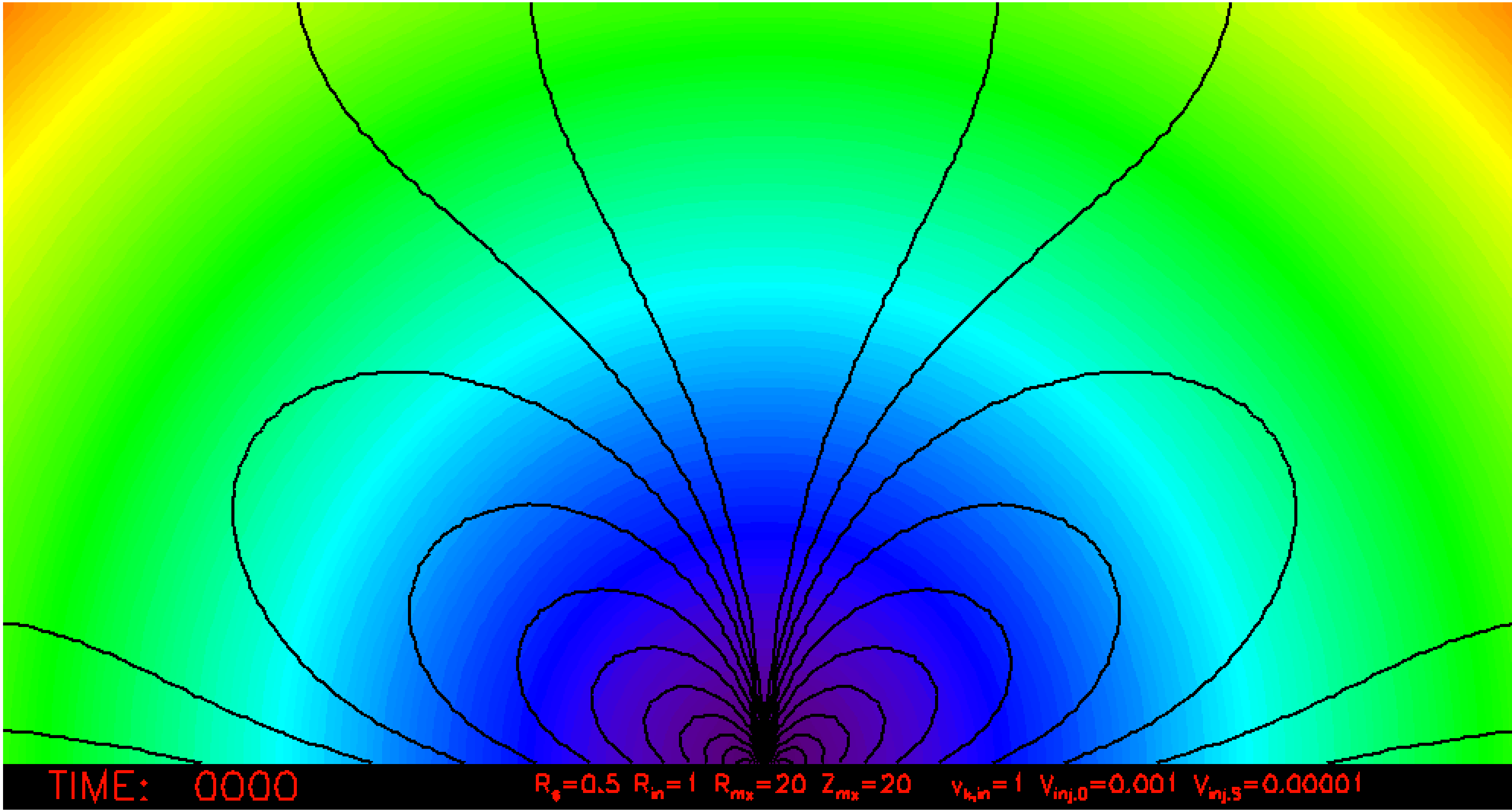

Disk wind

Slingshot effect:

Blandford & Payne (1982)

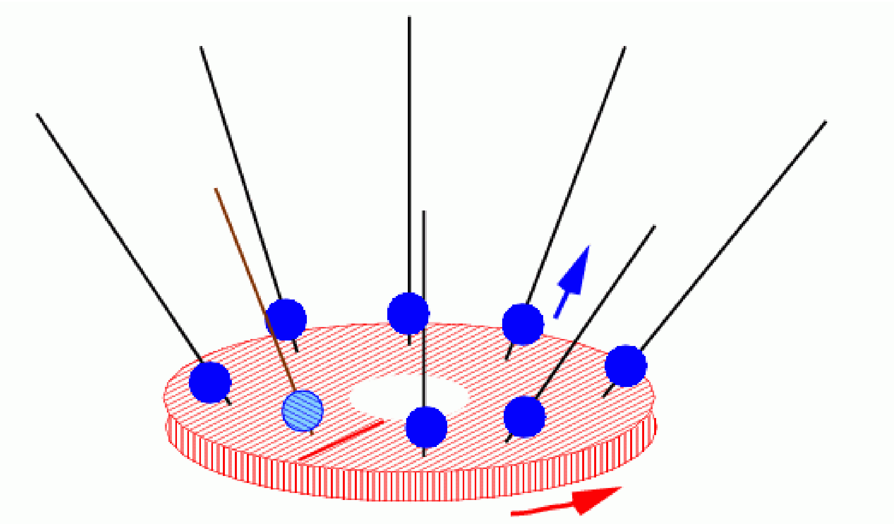

C. Fendt

•Gravitational potential:

$$\Phi = -\frac{GM}{\sqrt{r^2+z^2}}$$

•Effective gravitational potential along field line (incl. sling-shot effect):

$$\Phi = -\frac{GM}{r_0}\left[\frac{1}{2}\left(\frac{r}{r_0}\right)^2 + \frac{r_0}{\sqrt{r^2+z^2}}\right]$$

Disk wind

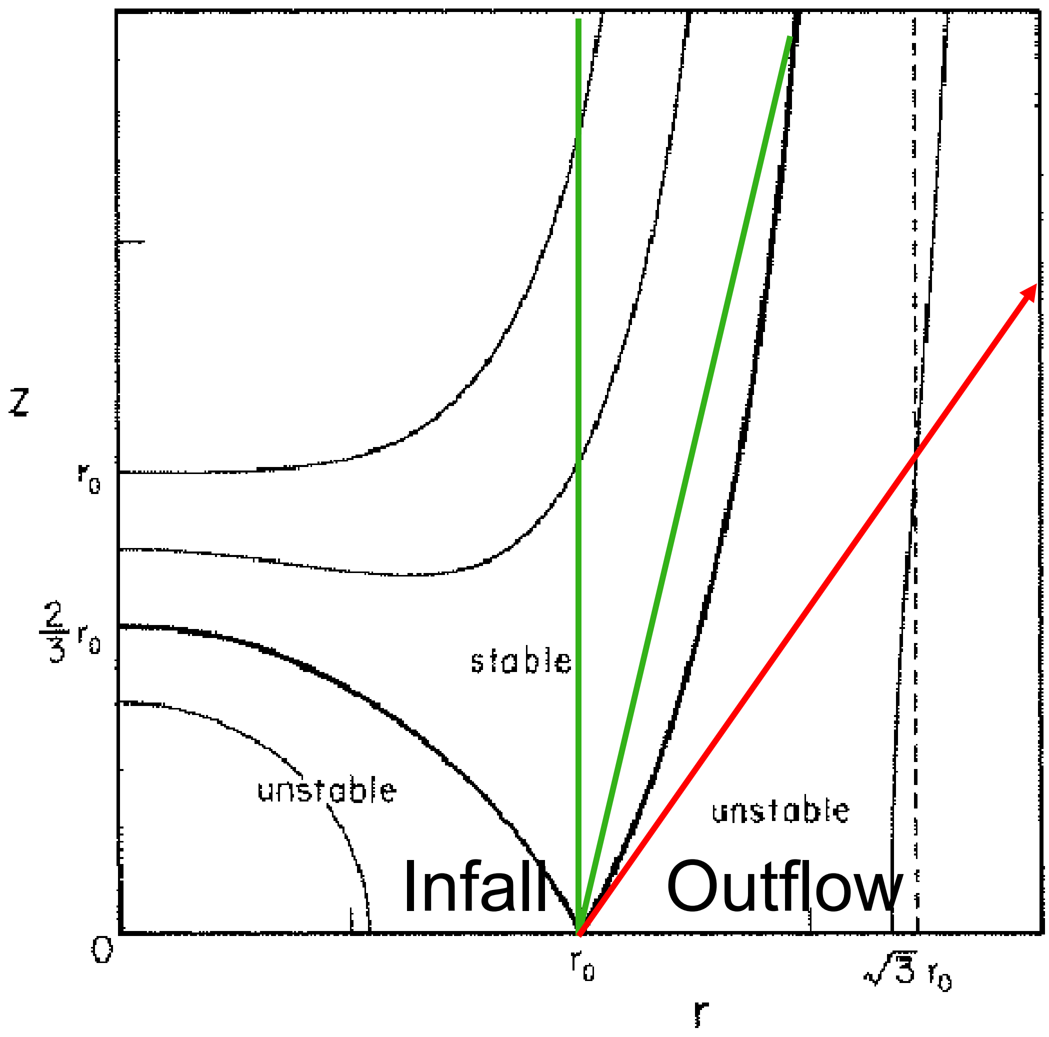

Critical angle:

60 degrees with disk plane.

Beyond that: outflow of matter.

Disk wind model

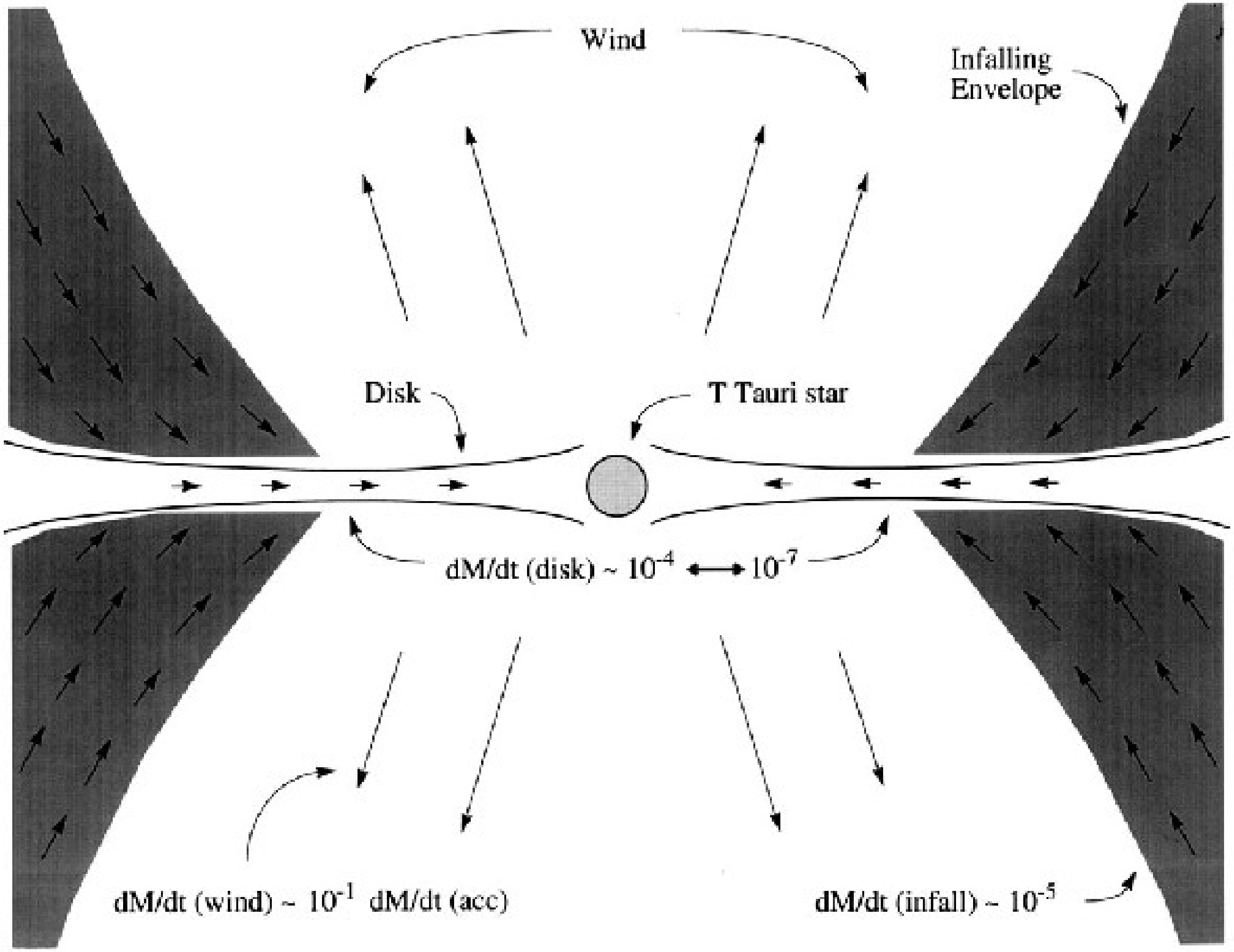

Figure 1 Schematic picture of FU Ori objects. FU Ori outbursts are caused by disk accretion increasing from $\sim 10^{-7}\ M_{\odot}\ \mathrm{yr}^{-1}$ to $\sim 10^{-4}\ M_{\odot}\ \mathrm{yr}^{-1}$, adding $\sim 10^{-2}\ M_{\odot}$ to the central T Tauri star during the event. Mass is fed into the disk by the remanant collapsing protostellar envelope with an infall rate $\lesssim 10^{-5}\ M_{\odot}\ \mathrm{yr}^{-1}$; the disk ejects roughly 10% of the accreted material in a high-velocity wind.

Consistent with FU Orionis out-bursts

Outflow size vs. distance

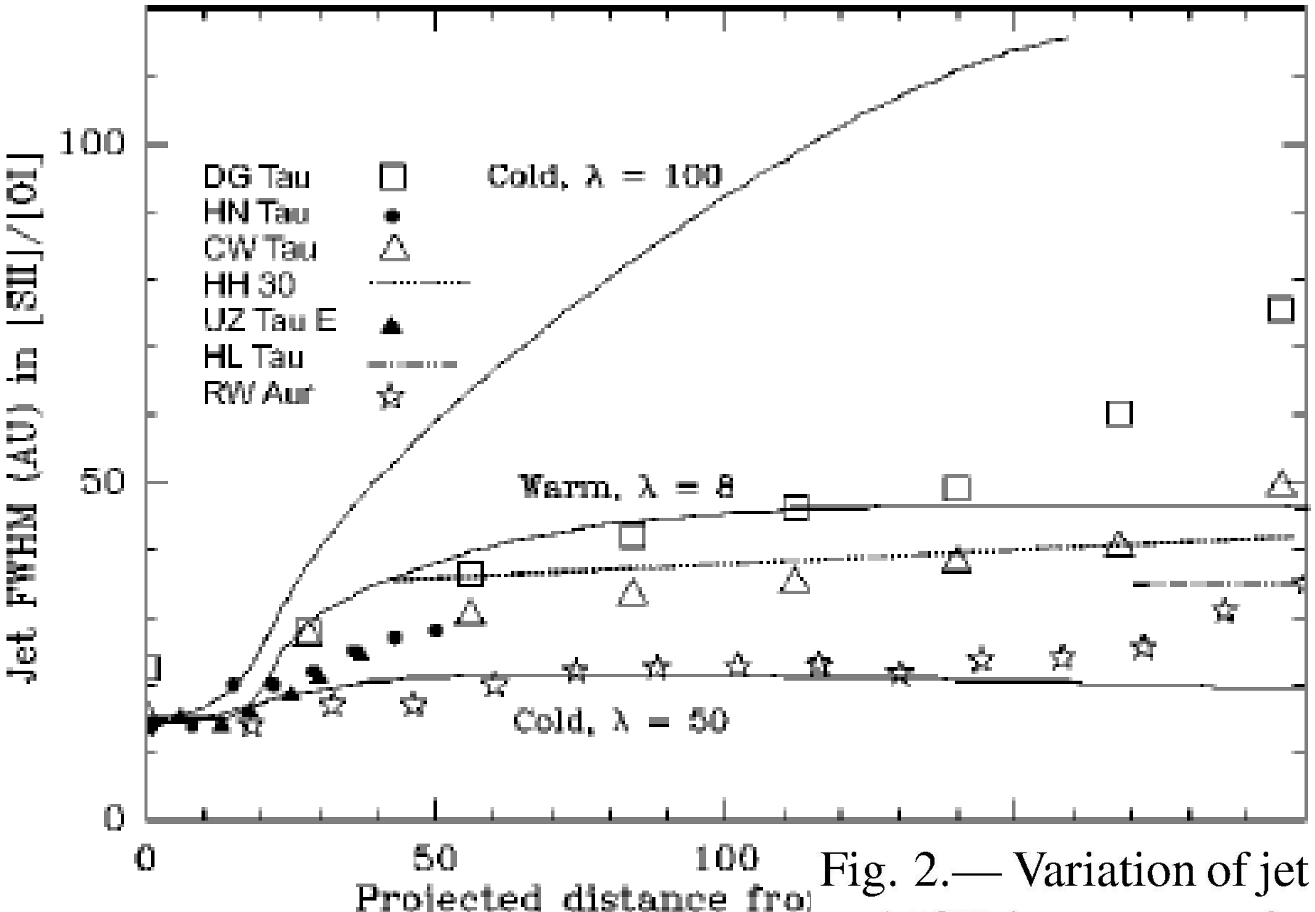

Ray et al. 2006, PPV

Fig. 2.— Variation of jet width (FWHM) derived from [SII] and [OI] images as a function of distance from the source. Data points are from CFHT/PUEO and HST/STIS observations made by the authors as well as those of *Hartigan et al.*, (2004). Overlaid (solid lines) are predicted variations based on two cold disk wind models with low efficiency (high λ) and a warm disk solution for comparison from *Dougados et al.*, (2004).

X-wind versus Disk-wind

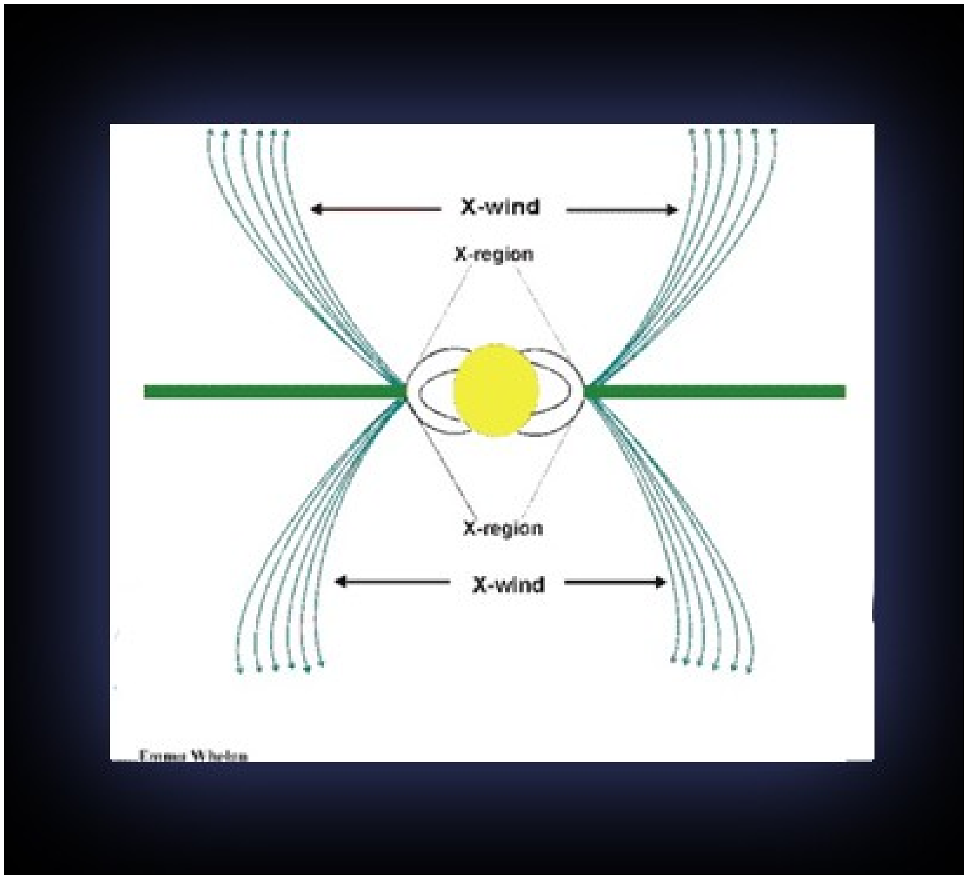

The X-wind model, the magnetic field of the star connects to the disk at the X-point. Here the accretion disk and star co-rotate and a wind, later collimated into a jet, is launched outwards along the open field lines.

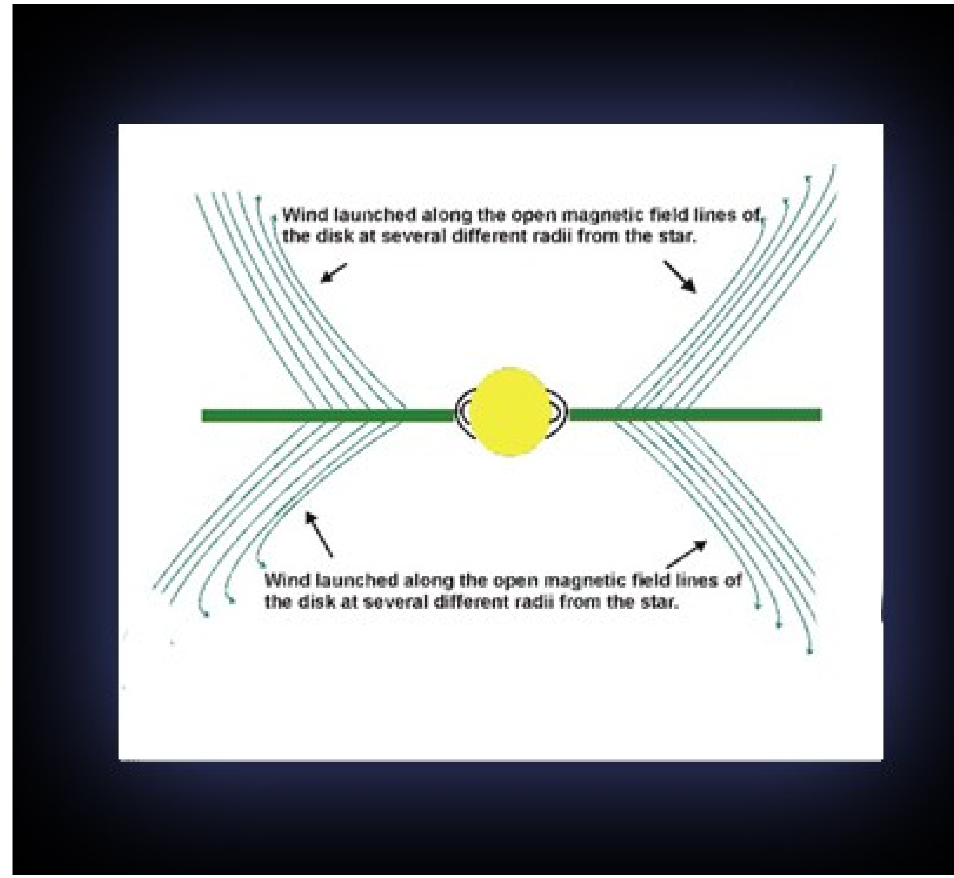

The disk-wind model, the wind is launched along the open field lines of the disk over a range of radii down to the co-rotation radius.

http://www.jetsets.org/collimationofjets.html

Collapse and outflow:
CO outflow as a "circulation solution"

Alternative model for outflow:
- central accretion-ejection engine for jet
+ global circulation pattern for CO flow

- Predict: CO outflow not due to jet entrainment.
I jet; II circulation region; III infalling envelope

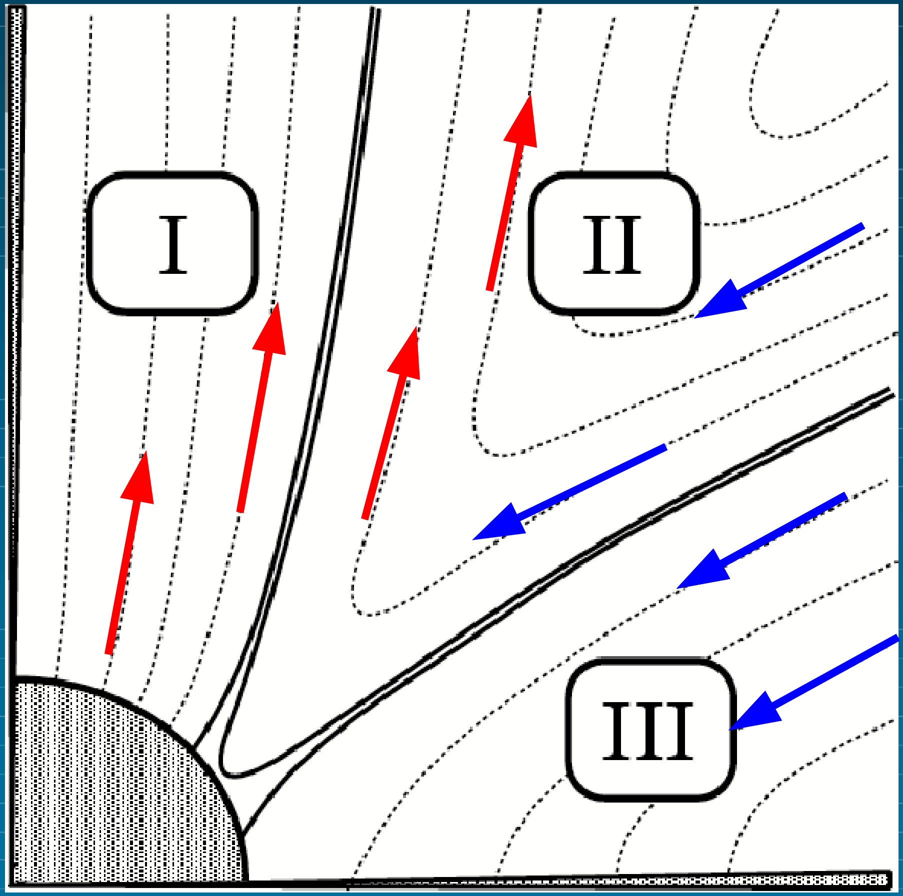

Lery et al (2002)

Different outflow models

Molecular outflow properties predicted by different models

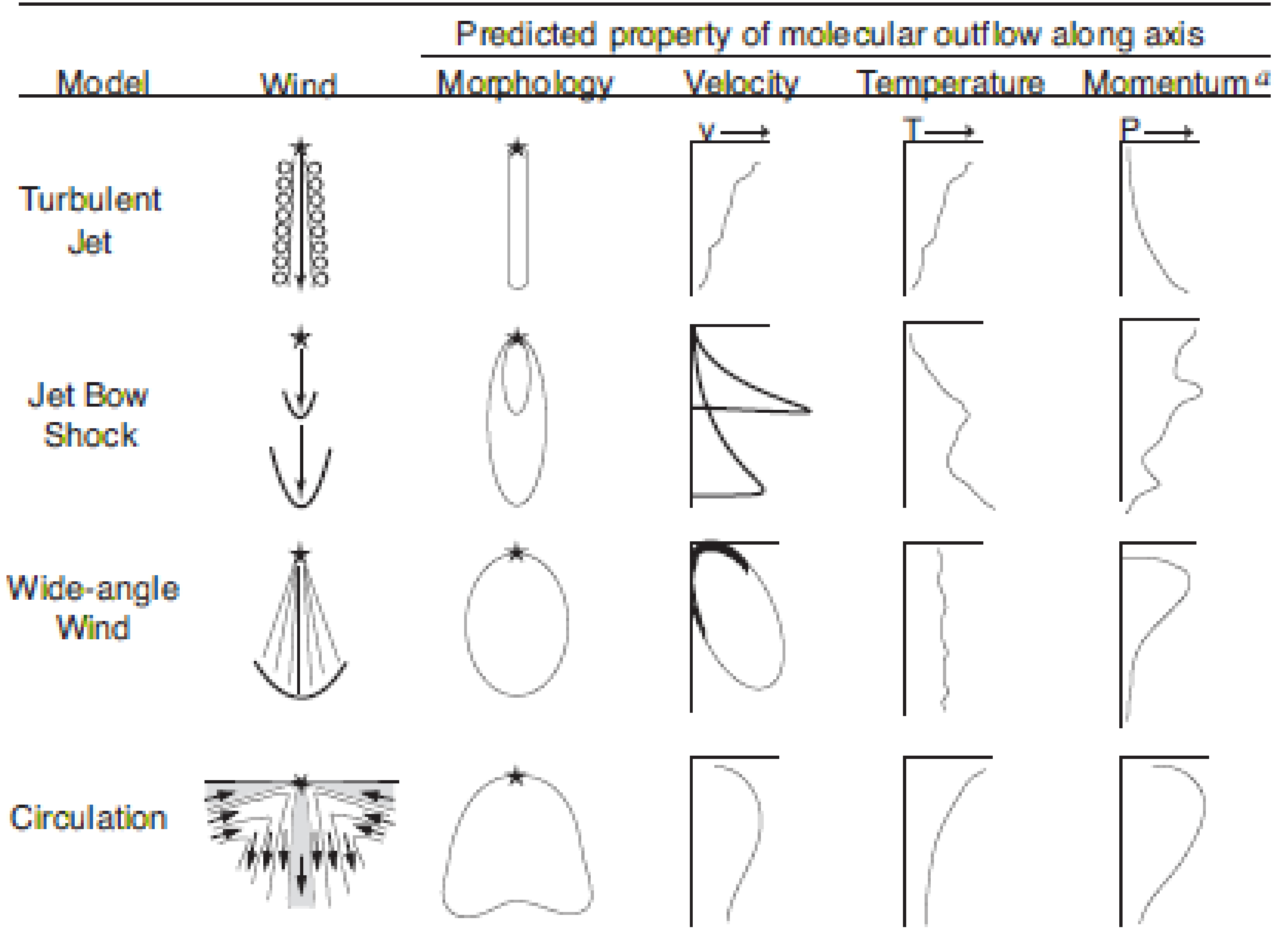

[a] Assuming an underlying density distribution of r^{-1} to r^{-2}.

Arce et al. 2006, PPV

Are jets really a way to get rid of angular momentum?

Detection of jet rotation!

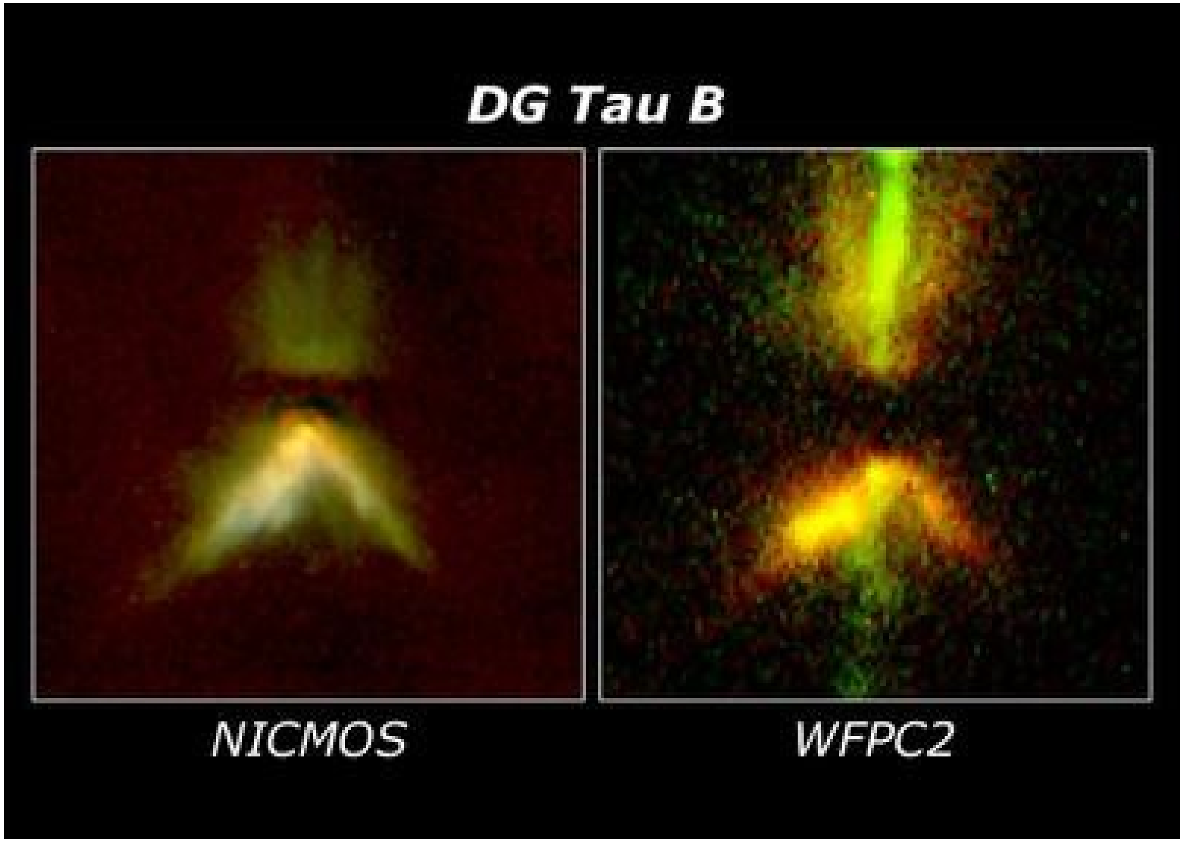

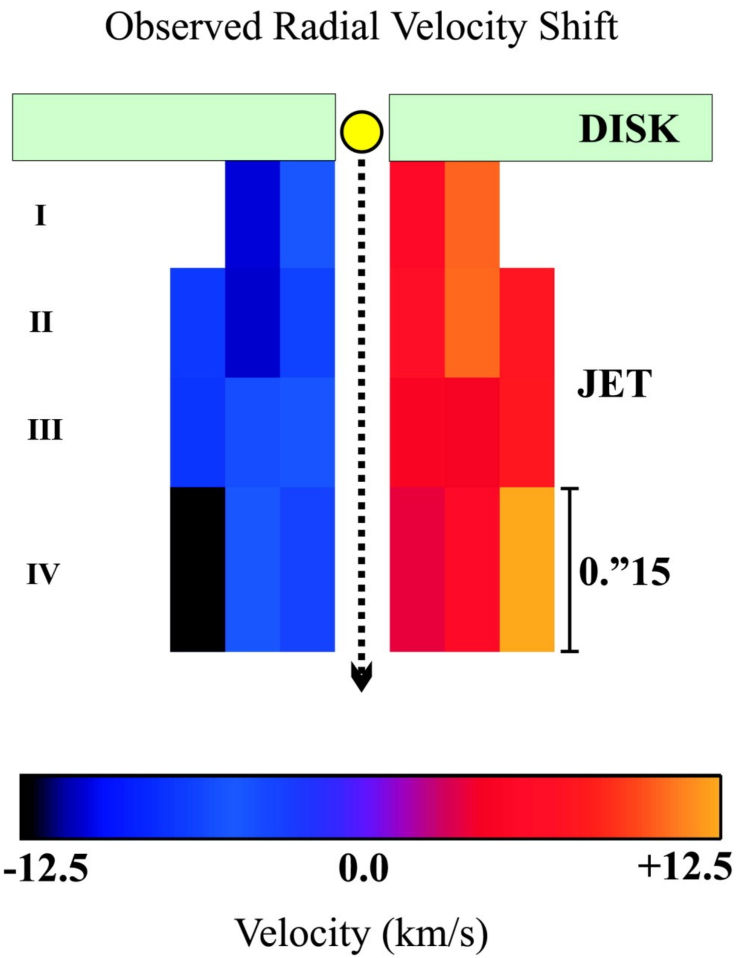

Bacciotti et al. 2002

Observational constraints

- Foot-print radius: undecided – some observations claim very small ones (down to 0.014 AU = 3 $R_\odot$ - would favor X-wind)

- Angular momentum of jet seems to be small – takes care of angular momentum problem of star, but disk has to look after itself

- Radial velocities and proper motions: 100-200 km/s for jets

→ Higher angular resolution needed to see detaching radius